Physics of Fluids

RESEARCH ARTICLE | MARCH 26 2024

Integrability, breather, rogue wave, lump, lump-multi-stripe, and lump-multi-soliton solutions of a (3 + 1)-dimensional nonlinear evolution equation

Uttam Kumar Mandal ; Amiya Das ; Wen-Xiu Ma

Physics of Fluids 36, 037151 (2024)
https://doi.org/10.1063/5.0195378

Physics of Fluids ARTICLE pubs.aip.org/aip/pof

Integrability, breather, rogue wave, lump, lump-multi-stripe, and lump-multi-soliton solutions of a (3 + 1)-dimensional nonlinear evolution equation

Cite as: Phys. Fluids **36**, 037151 (2024); doi: 10.1063/5.0195378
Submitted: 2 January 2024 · Accepted: 5 March 2024 ·
Published Online: 26 March 2024

View Online Export Citation CrossMark

Uttam Kumar Mandal,[1] Amiya Das,[1,b)] and Wen-Xiu Ma[2,3,4,5,a)]

AFFILIATIONS

[1]Department of Mathematics, University of Kalyani, Kalyani 741235, India
[2]Department of Mathematics, Zhejiang Normal University, Jinhua 321004, Zhejiang, China
[3]Department of Mathematics, King Abdulaziz University, Jeddah 21589, Saudi Arabia
[4]Department of Mathematics and Statistics, University of South Florida, Tampa, Florida 33620-5700, USA
[5]Material Science Innovation and Modelling, North-West University Mafikeng Campus, Private Bag X2046, Mmabatho 2735, South Africa

[a)]Author to whom correspondence should be addressed: mawx@cas.usf.edu
[b)]Electronic mail: amiya620@gmail.com and amiyamath18@klyuniv.ac.in

ABSTRACT

In this article, we consider a new $(3+1)$-dimensional evolution equation, which can be used to interpret the propagation of nonlinear waves in the oceans and seas. We effectively investigate the integrable properties of the considered nonlinear evolution equation through several aspects. First of all, we present some elementary properties of multi-dimensional Bell polynomial theory and its relation with Hirota bilinear form. Utilizing those relations, we derive a Hirota bilinear form and a bilinear Bäcklund transformation. By employing the Cole–Hopf transformation in the bilinear Bäcklund transformation, we present a Lax pair. Additionally, using the Bell polynomial theory, we compute an infinite number of conservation laws. Moreover, we obtain one-, two-, and three-soliton solutions explicitly from Hirota bilinear form and illustrate them graphically. Breather solutions are also derived by employing appropriate complex conjugate parameters in the two-soliton solution. Choosing the generalized algorithm for rogue waves derived from the N-soliton solution, we directly obtain a first-order center-controllable rogue wave. Lump solutions are formulated by employing a well-established quadratic test function as a solution to the Hirota bilinear form. Further taking the test function in a combined form of quadratic and exponential functions, we obtain lump-multi-stripe solutions. Furthermore, a combined form of quadratic and hyperbolic cosine functions produces lump-multi-soliton solutions. The fission and fusion effects in the evolution of lump-multi-stripe solutions and lump-soliton-solutions are demonstrated pictorially.

I. INTRODUCTION

In the past few decades, there has been a noticeable shift among researchers toward nonlinear models, driven by the rapid advancements in science and computer technology. Nonlinear evolution equations (NLEEs) play a pivotal role in describing a myriad of phenomena across various scientific disciplines, including physics, engineering, biology, and finance. These equations capture the complexity inherent in many natural processes, allowing for a more accurate representation of real-world dynamics like fluid mechanics,[1] optical fibers,[2] oceanography,[3] solid-state physics,[4] geochemistry,[5] plasma physics,[6] nonlinear optics,[7] and wave propagation in shallow water.[8] In recent years, there has been a notable focus on the exploration of constructing exact solutions for these nonlinear evolution equations (NLEEs) to enhance our understanding of their dynamical properties with greater accuracy. Due to the growing interest in nonlinear partial differential equations (NLPDEs), researchers are actively exploring a broader range of analytical and numerical methods to study them, leading to the computation of various novel types of exact solutions.[9–14] Studies on the integrability of nonlinear evolution equations become crucial for researchers, as it ensures the existence of exact solutions. While a precise definition of integrability is elusive, indicators such as the Hirota bilinear form,[15] inverse Scattering method,[16] Painlevè analysis,[17–19] bilinear neural network method,[20] bilinear Bäcklund transformation,[21] bilinear residual network method,[22] Lax pair,[23] Darboux transformation method,[24] Lie symmetry analysis,[25–27] infinite conservation laws,[28] etc. can effectively characterize integrability. Utilizing a Lax pair for a nonlinear system, a series of integrable properties, including Hamiltonian structures[29] and an infinite number of conserved quantities,[30] can be demonstrated. Among them, the Hirota bilinear method is one of the most conventional methods and recognized as a powerful approach for analyzing NLEEs. A pivotal aspect of this method involves expressing the original equation in a bilinear form. Upon formulating the bilinear representation of nonlinear evolution equations (NLEEs), one can directly acquire quasi-periodic wave solutions, rational solutions, multi-soliton solutions, and various other exact solutions through the utilization of the bilinear structure.[31–39] Kumar and Mohan recently proposed a systematic computational method to ascertain the bilinear form of nonlinear partial differential equations.[40] Using this method, it becomes straightforward to derive the Hirota bilinear form by employing symbolic computational software such as Mathematica, Maple, and Matlab. Lambert *et al.*[41–43] introduced an innovative approach for obtaining the Hirota bilinear form of nonlinear evolution equations (NLEEs) through the application of Bell polynomial theory. Through this approach, the bilinear Bäcklund transformation and Lax pair can be directly derived from the Hirota bilinear form. Fan[44] expanded upon this method to directly derive infinite conservation laws from the bilinear Bäcklund transformation. Lately, numerous researchers have utilized this approach to study the integrability of diverse types of nonlinear evolution equations (NLEEs) and have yielded a variety of exact solutions.[45–51] Researchers have shown a growing interest in the intriguing dynamical properties of exact solutions of nonlinear evolution equations (NLEEs), especially in phenomena such as solitons, lumps, breathers, and rogue waves. While waves travel through nonlinear media, variations in their amplitudes and widths are typically occur. Nevertheless, under specific conditions, the interaction between nonlinearity and dispersion can give a rise to the creation of enduring and localized waves, commonly referred to as solitons. A rogue wave also known as a giant wave is an exceptionally high wave that can manifest abruptly and vanish without a trace. These waves are localized both in space and time and were initially observed in the oceans.[52] The phenomenon of rogue waves has been experimentally verified in nonlinear optics, generated by the generalized nonlinear Schrödinger equation.[53] In recent years, rogue waves have been observed in various scientific research fields such as Bose–Einstein condensates,[54] superfluids,[55] plasma physics,[56] capillary flow,[57] nonlinear optical fibers,[58] and even in finance.[59] There are only a few methods available for computing rogue waves, and among them, the Darboux transform method[60–62] and the Hirota bilinear method[63–65] have been gaining significant popularity. Recently, Zhaqilao[66] proposed a systematic approach for computing higher-order center-controlled rogue waves based on the N-soliton solution. Utilizing this methodology, researchers have derived higher-order center controlled rogue waves for a variety of nonlinear evolution equations.[67–71] A breather solution is a type of partially localized solution characterized by a periodic structure in a specific direction. Breather solutions can be categorized into three types: Akhmediev breathers, Kuznetsov–Ma breathers, and Peregrine solitons. Breather of NLEEs can be obtained by using some standard methods like the Darboux transform method,[72] the Riemann–Hilbert approach,[30,73] and the Hirota bilinear method.[64] Lump solution is also a rational type solution and localized in all direction. Lump solution[74] of NLLEEs can be obtained directly by taking the quadratic function as a solution into the Hirota bilinear form of that equation. Numerous researchers worldwide have successfully obtained lump solutions for various nonlinear evolution equations using this method.[75–78] Recently, Ma *et al.* obtained a new type of lump solution using the Hirota bilinear method for the generalized Calogero–Bogoyavlenskii–Schiff equation.[76] The exploration of the dynamic interplay between lump solutions and various exact solutions such as soliton, kink, breather, etc. has emerged as a highly active area of research among researchers.[79,80] Lü and Chen[81] establish a necessary and sufficient condition for obtaining lump-multi-stripe and lump-multi-soliton solution with the help of Hirota bilinear form. Utilizing these theorem, they briefly analyze the dynamical behavior of lump-multi-stripe solution and lump-multi-soliton solution of three different $(2+1)$-dimensional nonlinear evolution equations. Lü and Chen[82] additionally establish a necessary and sufficient condition for determining lump-multi-kink solutions of nonlinear evolution equations (NLEEs) that exhibit a specific type of Hirota bilinear form. Furthermore, Mandal *et al.*[83] generalize the Lü's theorem and illustrate the evolution of lump-multi-kink solution for $(3+1)$-dimensional negative order KdV–CBS equation.

Recently, Akinyemi proposed a new $(2+1)$-dimensional evolution equation[84]

$$A\,u_{xt} + a u_{xx} + b\,(u^2)_{xx} + c u_{xxxx} + d\,u_{yy} = 0, \tag{1}$$

where a, b, and c are arbitrary real constants. Equation (1) describes the motion of water characterized by small-amplitude and long waves. Additionally, this mathematical model emphasizes few real life phenomenon such as tsunamis and tidal oscillations. Akinyemi shown that Eq. (1) is Painlevè integrable and derived various exact solutions. Wazwaz extend Eq. (1) to the following new $(3+1)$-dimensional equation:[85]

$$\begin{aligned} &u_{xt} + a u_{xx} + b\,(u^2)_{xx} + c\,u_{xxxx} + d\,u_{yy} + \alpha u_{xy} \\ &\quad + \beta\,u_{xz} + \gamma\,u_{yz} + \delta\,u_{zz} = 0, \end{aligned} \tag{2}$$

where a, b, c, d, α, β, γ, and δ are arbitrary real constants. Equation (2) finds utility in the representation and analysis of the intricate dynamics governing wave propagation in oceans and seas, offering noteworthy prospects for applications in fluid mechanics, plasma physics, and allied fields. In Ref. 85, Wazwaz shown that Eq. (2) also passes the Painlevè integrability test and studied multiple soliton solutions and lump solutions.

We observed a gap in the existing literature regarding the investigation of the bilinear Bäcklund transformation, Lax pair, and infinite conservation laws for Eq. (2). This observation motivated us to study these aspects in the current exposition. Our primary objective in this article is to explore the integrability and exact solutions of the nonlinear evolution described by Eq. (2).

The organization of our article is as follows. In Sec. II, we present some elementary properties of Bell polynomial theory and their relation with Hirota D-operator. Section III is entirely dedicated to examining the Hirota bilinear form, bilinear Bäcklund transformation, and associated Lax pair formulation of Eq. (2) through the utilization of Bell Polynomial theory. In Sec. IV, we derive infinitely many conservation laws. In Sec. V, we calculate one-, two-, and three-soliton solution and present their evolution graphically. In Sec. VI, we derive first order breather solution. In Sec. VII, we explore first order center controlled rogue wave of Eq. (2). In Sec. VIII, we obtain lump solution of the considered equation. Sections IX and X are exclusively focused on computing the lump-multi-stripe solution and lump-multi-soliton solution as well as analyzing their dynamic behavior. In Sec. XI, we have depicted the obtained solutions and discussed their propagation and nonlinear interaction with other solutions elaborately. Finally, in Sec. XII, we draw conclusions based on our work.

II. MULTI-DIMENSIONAL BELL POLYNOMIALS

In this section, we provide a brief overview of the fundamental principles and representations of Bell polynomials.[41,42] Assume η is a C^∞ function of t. The one-dimensional Bell polynomial, as defined in Ref. 41, is expressed as

$$Y_{nt}(\eta) = Y_n(\eta_1, \eta_2, \ldots, \eta_{nt}) = e^{-\eta}\partial_t{}^n e^{\eta}, \quad n = 1, 2, 3, \ldots. \tag{3}$$

Several one-dimensional Bell polynomials can be derived from the aforementioned statement as

$$Y_t = \eta_t,\ Y_{2t} = \eta_{2t} + \eta_t{}^2, \quad Y_{3t} = \eta_{3t} + 3\eta_t\eta_{2t} + \eta_t{}^3, \ldots. \tag{4}$$

We use the formula

$$Y_{nt}(\eta) = \sum \frac{n!}{a_1!a_2!\ldots a_n!}\left(\frac{\eta_t}{1!}\right)^{a_1}\left(\frac{\eta_{2t}}{2!}\right)^{a_2}\cdots\left(\frac{\eta_{nt}}{n!}\right)^{a_n}, \tag{5}$$

where the sum runs over all partitions of $n = a_1 + 2a_2 + \cdots + na_n$ and obtains the aforementioned expressions, Eq. (4). Assuming $\eta = \eta(t_1, t_2, \ldots, t_s)$ as a C^∞ multi-variable function, we can extend the dimension of the Bell polynomial. The multi-dimensional Bell polynomial can then be expressed as follows:

$$Y_{n_1t_1,\ldots,n_st_s}(\eta) \equiv Y_{n_1,\ldots,n_s}(\eta_{m_1t_1,\ldots,m_st_s}) = e^{-\eta}\partial_{t_1}^{n_1}\ldots\partial_{t_s}^{n_s}e^{\eta}, \tag{6}$$

where $\eta_{m_1t_1,\ldots,m_st_s} = \partial_{t_1}^{m_1}\ldots\partial_{t_s}^{m_s}\eta, m_i = 0, 1, \ldots, n_i,$ and $i = 1, 2, \ldots, s$. Here, $Y_{n_1t_1,\ldots,n_st_s}(\eta)$ denotes the multi-variable Bell polynomial with respect to $\eta_{m_1t_1,\ldots,m_st_s}$. Specifically, if we select η as a function of both t and z, the corresponding lower-order two-dimensional Bell polynomials can be derived as follows:

$$Y_{2t(\eta)} = \eta_{2t} + \eta_t^2, \quad Y_{3t(\eta)} = \eta_{3t} + 3\eta_{2t}\eta_t + \eta_t^3, \tag{7}$$

$$Y_{t,z} = \eta_{t,z} + \eta_t\eta_z, \quad Y_{2t,z}(\eta) = \eta_{2t,z} + \eta_{2t}\eta_z + 2\eta_{t,z}\eta_t + \eta_t^2\eta_z, \ldots. \tag{8}$$

According to the aforementioned one-dimensional Bell polynomials, Eq. (6), we can depict multi-dimensional binary Bell polynomials as follows:

$$\mathscr{Y}_{n_1t_1,\ldots,n_st_s}(\mathscr{f}, \mathscr{g}) = Y_{n_1t_1,\ldots,n_st_s}(\eta), \tag{9}$$

where

$$\eta_{m_1t_1,\ldots,m_st_s} = \begin{cases} \mathscr{f}_{m_1t_1,\ldots,m_st_s}, & m_1 + \cdots + m_s \text{ is odd}, \\ \mathscr{g}_{m_1t_1,\ldots,m_st_s}, & m_1 + \cdots + m_s \text{ is even}. \end{cases} \tag{10}$$

The following are a few two-dimensional binary Bell polynomials that can be derived from the above-mentioned statement:

$$\begin{gathered} \mathscr{Y}_t(\mathscr{f}) = \mathscr{f}_t, \mathscr{Y}_{2t}(\mathscr{f}, \mathscr{g}) = \mathscr{g}_{2t} + \mathscr{f}_t^2, \\ \mathscr{Y}_{t,z}(\mathscr{f}, \mathscr{g}) = \mathscr{g}_{t,z} + \mathscr{f}_t\mathscr{f}_z, \\ \mathscr{Y}_{2t,z}(\mathscr{f}, \mathscr{g}) = \mathscr{f}_{2t,z} + \mathscr{g}_{2t}\mathscr{f}_z + 2\mathscr{g}_{t,z}\mathscr{f}_t + \mathscr{f}_t^2\mathscr{f}_z, \\ \mathscr{Y}_{3t} = \mathscr{f}_{3t} + 3\mathscr{g}_{2t}\mathscr{f}_t + \mathscr{f}_t^3, \ldots. \end{gathered} \tag{11}$$

With the help of the identity

$$(\eta\psi)^{-1}D_{t_1}^{n_1}\ldots D_{t_s}^{n_s}\eta.\psi = \mathscr{Y}_{n_1t_1,\ldots,n_st_s}(\mathscr{f} = \ln\eta/\psi,\ \mathscr{g} = \ln\eta\psi), \tag{12}$$

we can establish a relation between the conventional Hirota bilinear expression $D_{t_1}^{n_1}\ldots D_{t_s}^{n_s}\eta.\psi$ and binary Bell polynomials, where the D-operator is presented by Hirota[15] as follows:

$$\begin{aligned} D_{t_1}^{n_1}\ldots D_{t_s}^{n_s}\eta.\psi = (\partial_{t_1} - \partial_{t_1'})^{n_1}\ldots(\partial_{t_s} - \partial_{t_s'})^{n_s}\eta(t_1, \ldots, t_s) \\ \cdot\psi(t_1', \ldots t_s')|_{t_1'=t_1,\ldots,t_s'=t_s}. \end{aligned}$$

In case when $\eta = \psi$, the identity Eq. (12) becomes

$$\begin{aligned} (\eta)^{-2}D_{t_1}^{n_1}\ldots D_{t_s}^{n_s}\eta.\eta &= \mathscr{Y}_{n_1t_1,\ldots,n_st_s}(\mathscr{f} = 0, \mathscr{g} = 2\ln\eta) \\ &= \begin{cases} 0, & n_1 + \cdots + n_s \text{ is odd}, \\ \mathscr{P}_{n_1t_1,\ldots,n_st_s}(\mathscr{p}), & n_1 + \cdots + n_s \text{ is even}. \end{cases} \end{aligned} \tag{13}$$

Here, the $\mathscr{P}$-polynomials refer to the even-ordered $\mathscr{Y}$-polynomials, and a few of the initial ones are listed as follows:

$$\begin{gathered} \mathscr{P}_{2t}(\mathscr{p}) = \mathscr{p}_{2t}, \quad \mathscr{P}_{t,z}(\mathscr{p}) = \mathscr{p}_{t,z}, \\ \mathscr{P}_{3t,z}(\mathscr{p}) = \mathscr{p}_{3t,z} + 3\mathscr{p}_{t,z}\mathscr{p}_{2t}, \quad \mathscr{P}_{4t}(\mathscr{p}) = \mathscr{p}_{4t} + 3\mathscr{p}_{2t}^2. \end{gathered} \tag{14}$$

The binary Bell polynomial $\mathscr{Y}_{n_1t_1,\ldots,n_st_s}(\mathscr{f}, \mathscr{g})$ can be written as a linear combination of $\mathscr{P}$-polynomials and Bell polynomials $Y_{n_1t_1,\ldots,n_st_s}(\mathscr{f})$ as

$$(\eta\psi)^{-1}D_{t_1}^{n_1}\ldots D_{t_s}^{n_s}\eta.\psi = \mathscr{Y}_{n_1t_1,\ldots,n_st_s}(\mathscr{f}, \mathscr{g}),$$

where

$$\mathscr{f} = \ln\eta/\psi \quad \text{and} \quad \mathscr{g} = \ln\eta\psi = \mathscr{Y}_{n_1t_1,\ldots,n_st_s}(\mathscr{f}, \mathscr{f} + \mathscr{p}),$$

where

$$\begin{aligned} &\mathscr{f} = \ln\eta/\psi \quad \text{and} \quad \mathscr{p} = 2\ln\psi \\ &= \sum_{m_1=0}^{n_1}\cdots\sum_{m_s=0}^{n_s}\prod_{i=1}^{s}\binom{n_i}{m_i}\mathscr{P}_{m_1t_1,\ldots,m_st_s}(\mathscr{p})\,Y_{(n_1-m_1)t_1,\ldots,(n_s-m_s)t_s}(\mathscr{f}). \end{aligned} \tag{15}$$

Using Hopf–Cole transformation $\mathscr{f} = \ln\psi$, binary Bell polynomial can be expressed in the following form:

$$Y_{n_1t_1,\ldots,n_st_s}(\mathscr{f} = \ln\psi) = \frac{\psi_{n_1t_1,\ldots,n_st_s}}{\psi}, \tag{16}$$

through which, Eq. (15) can be reexpressed as

$$\begin{aligned} &(\eta\psi)^{-1}D_{t_1}^{n_1}\ldots D_{t_s}^{n_s}\eta.\psi \\ &= \psi^{-1}\sum_{m_1=0}^{n_1}\cdots\sum_{m_s=0}^{n_s}\prod_{i=1}^{s}\binom{n_i}{m_i}\mathscr{P}_{m_1t_1,\ldots,m_st_s}(\mathscr{p})\,\psi_{(n_1-m_1)t_1,\ldots,(n_s-m_s)t_s}. \end{aligned} \tag{17}$$

Equation (17) provides the most straightforward approach to constructing the associated Lax pair for the relevant nonlinear evolution equation. The Bell polynomial theory concepts mentioned earlier will be further employed to establish the bilinear form, bilinear Bäcklund transformation, and the Lax pair formulation of Eq. (2).

III. HIROTA BILINEAR FORM, BILINEAR BÄCKLUND TRANSFORMATION, AND LAX PAIR

In order to achieve Hirota bilinear form of Eq. (2), we introduce a new potential field q by setting

$$u = \frac{3c}{b} q_{xx}. \tag{18}$$

Substituting Eq. (18) in Eq. (2) and integrate twice it with respect to x yields

$$E(\mathscr{q}) = \mathscr{q}_{xt} + a\mathscr{q}_{2x} + c(\mathscr{q}_{4x} + 3\mathscr{q}_{2x}^2) + d\mathscr{q}_{2y} + \alpha\mathscr{q}_{xy} + \beta\mathscr{q}_{xz} + \gamma\mathscr{q}_{yz} + \delta\mathscr{q}_{2z} = 0. \tag{19}$$

Furthermore, we choose $\mathscr{q} = 2\log f$, and we deduce the Hirota bilinear of Eq. (2) by using the relation between P-polynomial and Hirota D-operator as

$$(D_xD_t + aD_x^2 + cD_x^4 + dD_y^2 + \alpha D_xD_y + \beta D_xD_z + \gamma D_yD_z + \delta D_z^2) f\cdot f = 0. \tag{20}$$

To formulate bilinear Bäcklund transformation, we choose $\mathscr{q}' = 2\log f'$ as a distinct solution of Eq. (2). Furthermore, we introduce two new variables $v = \frac{\mathscr{q}'-\mathscr{q}}{2}$ and $v = \frac{\mathscr{q}'+\mathscr{q}}{2}$. Then, the corresponding two-field condition can be written as

$$\begin{aligned} E(\mathscr{q}') - E(\mathscr{q}) &= 2[v_{xt} + av_{2x} + c(v_{4x} + 6v_{2x}w_{2x}) + dv_{2y} + \alpha v_{xy} + \beta v_{xz} + \gamma v_{yz} + \delta v_{2z}] \\ &= 2\frac{\partial}{\partial x}[\mathscr{Y}_t(v) + c\mathscr{Y}_{3x}(v\mathrm{w}) + \beta\mathscr{Y}_z(v)] + 2\mathscr{R}(v,w), \end{aligned} \tag{21}$$

where $\mathscr{R}(v,w) = av_{2x} + dv_{2y} + \alpha v_{xy} + \gamma v_{yz} + \delta v_{2z} + 3c$ Wronskisan $[\mathscr{Y}_{2x}(v,w), \mathscr{Y}_x(v)]$. In order to write $\mathscr{R}(v,w)$ in the expression of $\mathscr{Y}$ polynomials, we introduce a constraint as follows:

$$\mathscr{Y}_{2x}(v,w) + A\,\mathscr{Y}_z(v,w) = \eta, \tag{22}$$

where A is an undetermined constant and η is an arbitrary parameter.

Taking $3cA^2 = \delta$, $\mathscr{R}(v,w)$ can be written as

$$\mathscr{R}(v,w) = \frac{\partial}{\partial x}[(3c\eta + a)\mathscr{Y}_x(v) - 3cA\mathscr{Y}_{xz}(v,w)] + \frac{\partial}{\partial y}\left[\alpha\mathscr{Y}_x(v) + \gamma\mathscr{Y}_z(v) + d\mathscr{Y}_y(v)\right]. \tag{23}$$

Finally, Eq. (21) can be written as

$$\begin{aligned} E(\mathscr{q}') - E(\mathscr{q}) = {} & 2\frac{\partial}{\partial x}[\mathscr{Y}_t(v) + c\,\mathscr{Y}_{3x}(v,w) + \beta\mathscr{Y}_z(v) \\ & + (3c\eta + a)\mathscr{Y}_x(v) - 3cA\mathscr{Y}_{x,z}(v,w)] \\ & + 2\frac{\partial}{\partial y}[\alpha\mathscr{Y}_x(v) + d\mathscr{Y}_y(v) + \gamma\mathscr{Y}_z(v)]. \end{aligned} \tag{24}$$

Decoupling Eq. (24), we obtain the bilinear Bäcklund transformation of Eq. (2) as follows:

$$\mathscr{Y}_{2x}(v,w) + A\,\mathscr{Y}_z(v,w) = \eta, \tag{25a}$$

$$\mathscr{Y}_t(v) + c\mathscr{Y}_{3x}(v,w) + \beta\mathscr{Y}_z(v) + (3c\eta + a)\mathscr{Y}_x(v) - 3cA\mathscr{Y}_{x,z}(v,w) = \eta_1, \tag{25b}$$

$$\alpha\mathscr{Y}_x(v) + d\mathscr{Y}_y(v) + \gamma\mathscr{Y}_z(v) = \eta_2. \tag{25c}$$

With the help of Eq. (12), the aforesaid bilinear Bäcklund transformation Eq. (25) also can be written in terms of Hirota D-operator as follows:

$$(f'\cdot f)^{-1}\left[D_x^2 + AD_z - \eta\right](f'\cdot f) = 0, \tag{26a}$$

$$(f'\cdot f)^{-1}\left[D_t + cD_x^3 + \beta D_z + (3c\eta + a)D_x - 3cAD_xD_z - \eta_1\right](f'\cdot f) = 0, \tag{26b}$$

$$(f'\cdot f)^{-1}\left[\alpha D_x + dD_y + \gamma D_z - \eta_2\right](f'\cdot f) = 0. \tag{26c}$$

Using the Cole–Hopf transformation $v = \log\zeta$ and linearizing the Bell polynomial system, Eq. (25), we derive the Lax pair of Eq. (2) as

$$\zeta_{2x} + A\zeta_z + (q_{2x} - \eta)\zeta = 0, \tag{27a}$$

$$\zeta_t + \beta\zeta_z + c(\zeta_{xz} + \zeta_{3x} - 3A) + (a + 3c\eta + 3cq_{2x})\zeta_x - 3cAq_{xz}\zeta - \eta_1\zeta = 0, \tag{27b}$$

$$\alpha\zeta_x + d\zeta_y + \gamma\zeta_z - \eta_2\zeta = 0. \tag{27c}$$

IV. INFINITELY MANY CONSERVATION LAWS

To construct infinite conservation laws of Eq. (2), we rewrite Eqs. (22) and (24) in following form:

$$v_x^2 + Av_z - \eta = 0, \tag{28}$$

$$\frac{\partial}{\partial t}(v_x) + \frac{\partial}{\partial x}\left[c(v_{3x} + 3v_xw_{2x} + v_x^3) + (3c\eta + a)v_x - 3cAv_xv_z\right] + \frac{\partial}{\partial y}(\alpha v_x + dv_y + \gamma v_z) + \frac{\partial}{\partial z}(-3cA\eta + \delta v_z + 3cAv_x^2 + \beta v_z) = 0\,. \tag{29}$$

We present a novel potential function $\xi = \frac{\mathscr{q}_x' - \mathscr{q}_x}{2}$, which yields

$$v_x = \xi,\quad v_y = \partial_x^{-1}(\xi_y),\quad v_z = \partial_x^{-1}(\xi_z),\quad w_x = \mathscr{q}_x + \xi. \tag{30}$$

Substitution of Eq. (30) into Eq. (28) and Eq. (29) yields a Riccati type equation and a divergence type equation as

$$\xi^2 + \mathscr{q}_{2x} + \xi_x + A\partial_x^{-1}(\xi_z) - \eta = 0, \tag{31}$$

$$\begin{aligned} &\xi_t + \partial_x\left[c\xi_{2x} + 6c\xi\eta - 2c\xi^3 - 6cA\xi\partial_x^{-1}(\xi_z) + a\xi\right] \\ &\quad + \partial_z\left[-3cA\eta + \delta\partial_x^{-1}\xi_z + 3cA\xi^2 + \beta\partial_x^{-1}(\xi_z)\right] \\ &\quad + \partial y\left[\alpha\xi + d\partial_x^{-1}(\xi_y) + \gamma\partial_x^{-1}(\xi_z)\right] = 0. \end{aligned} \tag{32}$$

Setting $\eta = \xi^2$ and $\xi = \xi' + \epsilon$ in Eq. (31), we obtain

$$\mathscr{q}_{2x} + \xi_x' + 2\xi'\epsilon + \xi'^2 + A\partial_x^{-1}(\xi_z') - \epsilon^2 = 0. \tag{33}$$

We choose infinite series form of ξ' as

$$\xi' = \sum_{n=1}^{\infty} K_n(\mathscr{q}, \mathscr{q}_x, \mathscr{q}_{2x}, \ldots)\epsilon^{-n}. \tag{34}$$

Substituting Eq. (34) into Eq. (33) and equating all the like powers of ϵ, finally, we derive the recursions relations for the conserved densities as

$$K_1 = -\frac{1}{2}\varphi_{2x}, \tag{35a}$$

$$K_2 = -\frac{1}{2}\left[K_{1,x} + A\,\partial_x^{-1}(K_{1,z})\right] = \frac{1}{4}(\varphi_{3x} + A\,\varphi_{x,z}), \tag{35b}$$

$$K_3 = -\frac{1}{2}\left[K_{2,x} + A\partial_x^{-1}(K_{2,z}) + K_1^2\right] = -\frac{1}{8}\left[\varphi_{4x} + 2A(\varphi_{2xz} + \varphi_{2z})\varphi_{2x}^2\right], \tag{35c}$$

$$\cdots\cdots$$

$$K_{n+1} = -\frac{1}{2}\left(K_{n,x} + A\,\partial_x^{-1}K_{n,z} + \sum_{i=1}^{n-1}K_iK_{n-i}\right). \tag{35d}$$

Again substituting Eq. (34) with $\eta = \xi^2$ and $\xi = \xi' + \epsilon$ into Eq. (32), we have

$$\begin{aligned}&\sum_{n=1}^{\infty}K_{n,t}\epsilon^{-n} + \partial_x\Bigg[c\sum_{n=1}^{\infty}K_{n,2x}\epsilon^{-n} + 4c\epsilon^3 - 2c\left(\sum_{n=1}^{\infty}K_n\epsilon^{-n}\right)^3\\ &- 6c\epsilon\left(\sum_{n=1}^{\infty}K_n\epsilon^{-n}\right)^2 - 6cA\left(\sum_{n=1}^{\infty}K_n\epsilon^{-n}\right)\partial_x^{-1}\left(\sum_{n=1}^{\infty}K_{n,z}\epsilon^{-n}\right)\\ &+ a\left(\sum_{n=1}^{\infty}K_n\epsilon^{-n} + \epsilon\right)\Bigg] + \partial_y\Bigg[\alpha\left(\epsilon + \sum_{n=1}^{\infty}K_n\epsilon^{-n}\right)\\ &- 6c\epsilon + d\partial_x^{-1}\left(\sum_{n=1}^{\infty}K_{n,y}\epsilon^{-n}\right) + \gamma\partial_x^{-1}\left(\sum_{n=1}^{\infty}K_{n,z}\epsilon^{-n}\right)\Bigg]\\ &+ \partial_z\Bigg[3cA\left(\sum_{n=1}^{\infty}K_n\epsilon^{-n}\right)^2 + 6cA\left(\sum_{n=1}^{\infty}K_n\epsilon^{-n}\right)\epsilon\\ &+(\delta+\beta)\partial_x^{-1}\left(\sum_{n=1}^{\infty}K_{n,z}\epsilon^{-n}\right)\Bigg] = 0.\end{aligned} \tag{36}$$

Comparing the coefficient of all the like powers of ϵ from Eq. (36), we obtain the conservation laws of Eq. (2) as

$$K_{n,t} + \mathscr{L}_{n,x} + \mathscr{M}_{n,y} + \mathscr{N}_{n,z} = 0, \tag{37}$$

where

$$\mathscr{L}_1 = cK_{1,2x} + aK_1 - 6cK_1^2 - 6cA\partial_x^{-1}K_{2,z}, \tag{38a}$$

$$\mathscr{L}_2 = cK_{2,2x} + aK_2 - 12cK_1K_2 - 6cA(\partial_x^{-1}K_{3,z} + K_1\partial_x^{-1}K_{1,z}), \cdots\cdots \tag{38b}$$

$$\begin{aligned}\mathscr{L}_n = aK_n + c\left(K_{n,2x} - 6\sum_{i=1}^{n}K_iK_{n-i+1} - 2\sum_{i_1+i_2+i_3=n}K_{i_1}K_{i_2}K_{i_3}\right)\\ - 6cA\left(\partial_x^{-1}K_{n+1,z} + \sum_{n=1}^{n}K_i\partial_x^{-1}K_{n-i,y}\right),\end{aligned} \tag{38c}$$

$$\mathscr{M}_1 = \alpha K_1 + d\partial_x^{-1}K_{1,y} + \gamma\partial_x^{-1}K_{1,z}, \tag{39a}$$

$$\mathscr{M}_2 = \alpha K_2 + d\partial_x^{-1}K_{2,y} + \gamma\partial_x^{-1}K_{2,z}, \tag{39b}$$

$$\cdots\cdots$$

$$\mathscr{M}_n = \alpha K_n + d\partial_x^{-1}K_{n,y} + \gamma\partial_x^{-1}K_{n,z}, \tag{39c}$$

and

$$\mathscr{N}_1 = 6cAK_2 + (\beta+\delta)K_{1,z}, \tag{40a}$$

$$\mathscr{N}_2 = 6cAK_3 + 3cAK_1^2 + (\beta+\delta)K_{2,z}, \tag{40b}$$

$$\cdots\cdots$$

$$\mathscr{N}_n = 6cAK_{n+1} + 3cA\sum_{i=1}^{n-1}K_iK_{n-i} + (\beta+\delta)\partial_x^{-1}K_{n,z}. \tag{40c}$$

The recursion relations Eq. (35) provide the values of K_n.

V. SOLITON SOLUTIONS

A. One-soliton solution

To formulate one soliton solution of Eq. (2), we assume f in the following form:

$$f = 1 + e^{\Upsilon_1}, \tag{41}$$

where $\Upsilon_1 = k_1(x + p_1y + q_1z + w_1t) + \Upsilon_1^0$ and $k_1, p_1, q_1, \Upsilon_1^0$ are arbitrary constants. Substituting Eq. (41) into Eq. (20) and equating all exponential functions to zero, we obtain dispersion relation as

$$w_1 = -(a + c\,k_1^2 + d\,p_1^2 + \alpha\,p_1 + \beta\,q_1 + \gamma\,p_1q_1 + \delta\,q_1^2). \tag{42}$$

Finally, we obtain one-soliton solution of Eq. (2) by substituting Eq. (41) along with Eq. (42) into Eq. (20) as

$$u = \frac{6c}{b}\left[\log(1 + e^{\Upsilon_1})\right]_{2x}. \tag{43}$$

In Fig. 1, we present 3D plot, density plot, and 2D plot of one soliton solution Eq. (43), corresponding to parametric values as $a = c = d = \alpha = \beta = \gamma = \delta = 1,\ k_1 = 0.4,\ p_1 = 1.2,\ q_1 = 1.3,\ \Upsilon_1^0 = 0.$

B. Two-soliton solution

In order to obtain two soliton solution of Eq. (2), we choose f in the following form:

$$f = 1 + e^{\Upsilon_1} + e^{\Upsilon_2} + B_{12}e^{\Upsilon_1+\Upsilon_2}, \tag{44}$$

where $\Upsilon_i = k_i(x + p_iy + q_iz + w_it) + \Upsilon_i^0,\ (i = 1, 2)$ and $k_i, p_i, q_i, \Upsilon_i^0,\ (i = 1, 2)$ are arbitrary constants. Substituting Eq. (44) into Eq. (20), we derive dispersion relation and B_{12} as

$$w_i = -(a + c\,k_i^2 + d\,p_i^2 + \alpha\,p_i + \beta\,q_i + \gamma\,p_iq_i + \delta\,q_i^2),\ \ (i = 1, 2), \tag{45a}$$

$$B_{12} = \left[\frac{(k_1-k_2)(k_1w_1-k_2w_2) + (k_1-k_2)^2 + (k_1-k_2)^4 + (k_1p_1-k_2p_2)^2 + (k_1-k_2)(k_1p_1+k_1q_1-k_2p_2-k_2q_2) + (k_1p_1-k_2p_2)(k_1q_1-k_2q_2) + (k_1q_1-k_2q_2)^2}{(k_1+k_2)(k_1w_1+k_2w_2) + (k_1+k_2)^2 + (k_1+k_2)^4 + (k_1p_1+k_2p_2)^2 + (k_1+k_2)(k_1p_1+k_1q_1+k_2p_2+k_2q_2) + (k_1p_1+k_2p_2)(k_1q_1+k_2q_2) + (k_1q_1+k_2q_2)^2}\right]. \tag{45b}$$

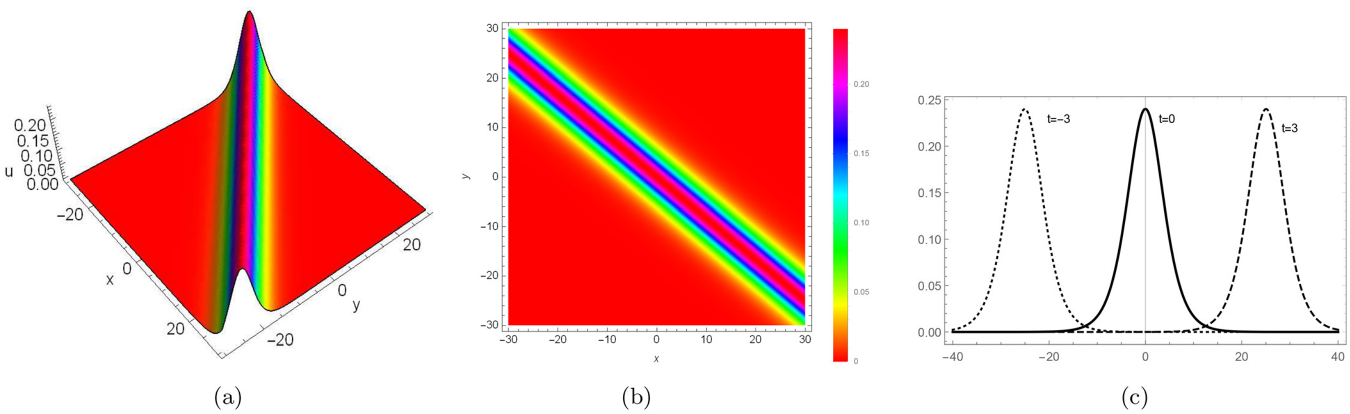

FIG. 1. One soliton solution of Eq. (2) given by Eq. (43). (a) 3D plot, (b) density plot, and (c) 2D plot at different times.

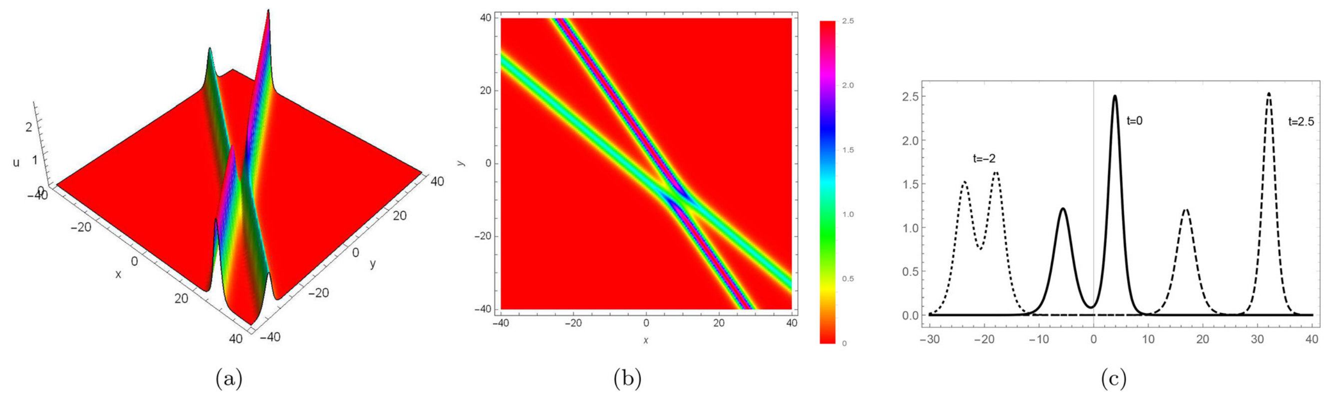

FIG. 2. Two soliton solution of Eq. (2) given by Eq. (46). (a) 3D plot, (b) density plot, and (c) 2D plot at different times.

Further substitution of Eq. (44) with Eq. (45) into Eq. (20) yields two soliton solution of Eq. (2) as

$$u = \frac{6c}{b}\left[\log(1 + e^{\Upsilon_1} + e^{\Upsilon_2} + B_{12}e^{\Upsilon_1+\Upsilon_2})\right]_{2x}. \tag{46}$$

In Fig. 2, we demonstrate 3D plot, density plot, and 2D plot of two soliton solution Eq. (46), corresponding to parametric values as $a = c = d = \alpha = \beta = \gamma = \delta = 1,\ \ k_1 = 0.9,\ \ p_1 = 1.2,\ \ q_1 = 1.3,$ $k_2 = -1.3, p_2 = 0.7, q_2 = 2$, and $\Upsilon_i^0 = 0\ (i = 1, 2)$.

C. Three-soliton solution

In similar way, we can derive three soliton solution of Eq. (2) by choosing f in the following form:

$$f = 1 + e^{\Upsilon_1} + e^{\Upsilon_2} + e^{\Upsilon_3} + B_{12}e^{\Upsilon_1+\Upsilon_2} + B_{13}e^{\Upsilon_1+\Upsilon_3} + B_{23}e^{\Upsilon_2+\Upsilon_3} + B_{123}e^{\Upsilon_1+\Upsilon_2\Upsilon_3}, \tag{47}$$

where $\Upsilon_i = k_i(x + p_i y + q_i z + w_i t) + \Upsilon_i^0,\ (i = 1, 2, 3)$ and $k_i, p_i, q_i, \Upsilon_i^0,\ (i = 1, 2, 3)$ are arbitrary constants. Substituting Eq. (47) into Eq. (20), we derive dispersion relation and B_{ij} as

$$w_i = -(a + c\,k_i^2 + d\,p_i^2 + \alpha\,p_i + \beta\,q_i + \gamma\,p_i q_i + \delta\,q_i^2),\quad (i = 1, 2, 3), \tag{48a}$$

$$B_{ij} = \left[\frac{(k_i - k_j)(k_i w_i - k_j w_j) + (k_i - k_j)^2 + (k_i - k_j)^4 + (k_i p_i - k_j p_j)^2 + (k_i - k_j)(k_i p_i + k_i q_i - k_j p_j - k_j q_j) + (k_i p_i - k_j p_j)(k_i q_i - k_j q_j) + (k_i q_i - k_j q_j)^2}{(k_i + k_j)(k_i w_i + k_j w_j) + (k_i + k_j)^2 + (k_i + k_j)^4 + (k_i p_i + k_j p_j)^2 + (k_i + k_j)(k_i p_i + k_i q_i + k_j p_j + k_j q_j) + (k_i p_i + k_j p_j)(k_i q_i + k_j q_j) + (k_i q_i + k_j q_j)^2}\right]. \tag{48b}$$

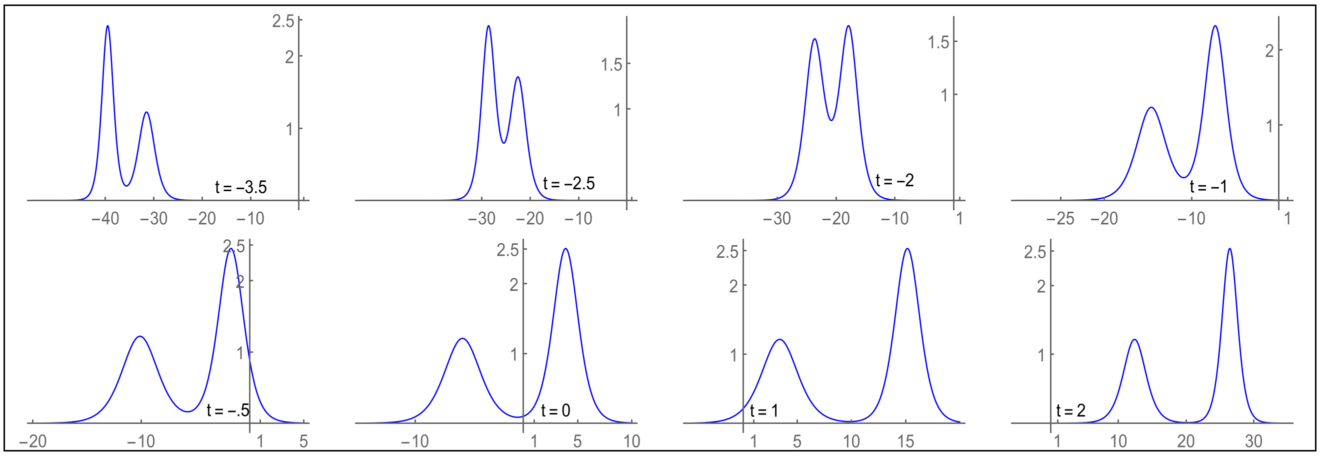

FIG. 3. Time evolution of two soliton solution of Eq. (2) for the same parameters as in Fig. 2.

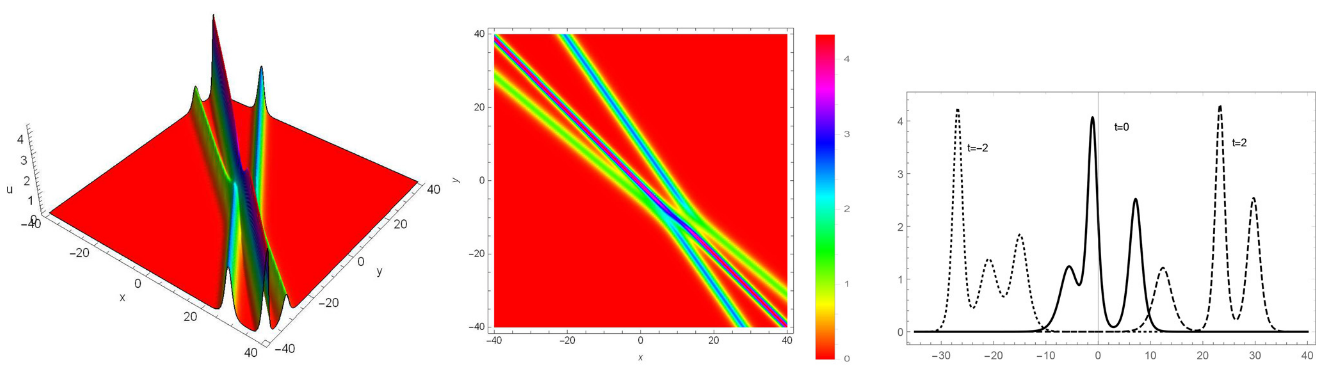

(a) (b) (c)

FIG. 4. Three soliton solution of Eq. (2) given by Eq. (49). (a) 3D plot, (b) density plot, and (c) 2D plot at different times.

Finally, substituting Eq. (47) with Eq. (48) into Eq. (20), we derive three soliton solution of Eq. (2) as

$$u = \frac{6c}{b}\big[\log(1 + e^{\Upsilon_1} + e^{\Upsilon_2} + e^{\Upsilon_3} + B_{12}e^{\Upsilon_1+\Upsilon_2} + B_{13}e^{\Upsilon_1+\Upsilon_3} + B_{23}e^{\Upsilon_2+\Upsilon_3} + B_{123}e^{\Upsilon_1+\Upsilon_2\Upsilon_3})\big]_{2x} \tag{49}$$

In Fig. 4, we illustrate three soliton solution graphically corresponding to the parametric values as $a = c = d = \alpha = \beta = \gamma = \delta = 1$, $k_1 = 0.9$, $p_1 = 1.2$, $q_1 = 1.3$, $k_2 = -1.3$, $p_2 = 0.7$, $q_2 = 2$, $k_3 = 1.7$, $p_3 = 1$, $q_3 = 1.7$, and $\Upsilon_i^0 = 0\ (i = 1, 2, 3)$.

VI. BREATHER SOLUTION

Utilizing the criteria outlined in prior studies[86,87] for acquiring breather solutions, one can derive an analytical expression for breather solutions by selecting appropriate parameters within the framework of the two-soliton solution. In order to derive the first-order breather solution, it is necessary to express the parameters in Eq. (44) in the following complex conjugate form:

$$k_1 = k_2^* = a + ib,\ \ p_1 = p_2^* = c + id,\ \ q_1 = q_2^* = e + if. \tag{50}$$

In particular, taking $k_1 = k_2^* = i$, $p_1 = p_2^* = 1$, $q_1 = q_2^* = 2 + i$, and $a = b = c = d = \alpha = \beta = \gamma = \delta = 1$, Eq. (44) can be written as

$$f = 1 + 2\cos(x + 2y + z + 6t)(\cosh(-2z - 10t) + \sinh(-2z - 10t)) - 2\cosh(-2z - 12t) - 2\sinh(-2z - 12t). \tag{51}$$

Substituting Eq. (51) into Eq. (20), we can obtain the first order breather solution of Eq. (2) as

$$u = 6[\log(1 + 2\cos(x + 2y + z + 6t)(\cosh(-2z - 10t) + \sinh(-2z - 10t)) - 2\cosh(-2z - 12t) - 2\sinh(-2z - 12t))]_{xx} \tag{52}$$

VII. ROGUE WAVE SOLUTION

In order to derive rogue wave solution of Eq. (2), we use the transformation $\rho = x + y - t$, which converts Eq. (2) into

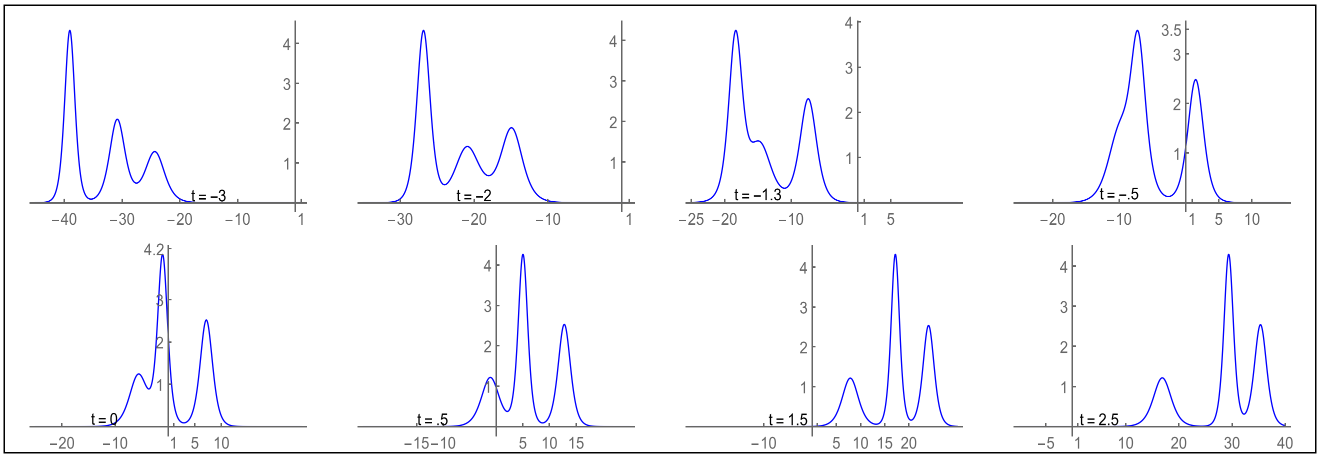

FIG. 5. Time evolution of three soliton solution of Eq. (2) for the same parameters as in Fig. 4.

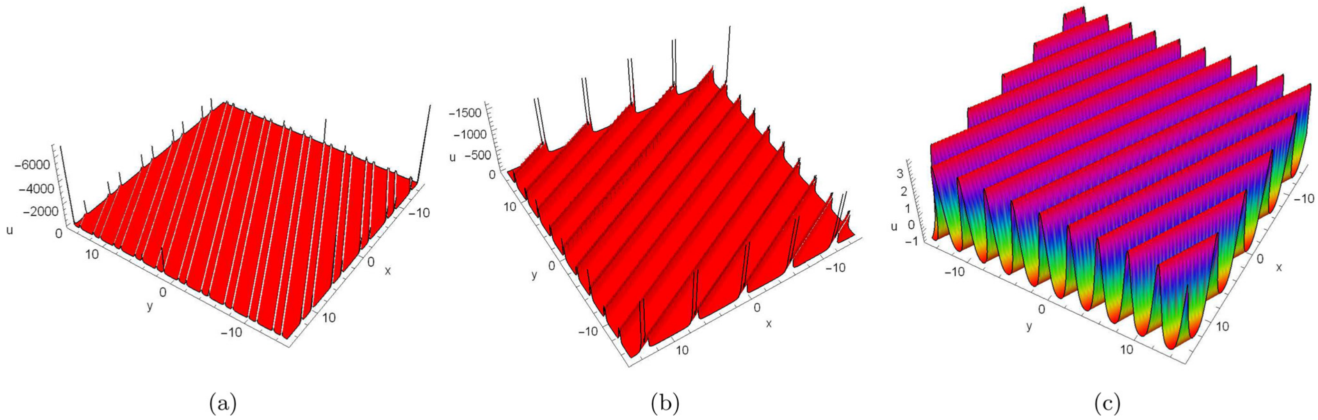

FIG. 6. Evolution of first order breather solution of Eq. (2) given by Eq. (52) at (a) $t=0$, (b) $t=0.165$, and (c) $t=0.3$.

$$(a+d+\alpha-1)u_{2\rho}+b(u^2)_{2\rho}+cu_{4\rho}+(\beta+\gamma)u_{\rho z}+u_{2z}=0. \quad (53)$$

Using the depending variable transformation

$$u(\rho,z)=\frac{3c}{b}[2\log g]_{\rho\rho}, \quad (54)$$

along with $c=-1$ and integrating twice with respect to ρ, we obtain Hirota bilinear equation corresponding to Eq. (53) as

$$\begin{aligned}&[(a+d+\alpha-1)D_\rho^2-D_\rho^4+(\beta+\gamma)D_\rho D_z+\delta D_z^2]g\cdot g\\&=(a+d+\alpha-1)(g\,g_{2\rho}-g_\rho^2)-(g_{4\rho}\,g-4g_\rho\,g_{2\rho}+3g_{2\rho}^2)\\&\quad+(\beta+\gamma)(g\,g_{\rho z}-g_\rho\,g_z)+\delta(g\,g_{2z}-g_z^2)=0. \quad (55)\end{aligned}$$

The generalized form of center controlled rogue wave solution[67] can be considered as

$$\begin{aligned}g(\rho,z)&=\tilde{g}_n(\rho,z,c_1,c_2)\\&=\sum_{j=0}^{\frac{n(n+1)}{2}}\sum_{i=0}^{j}b_{n(n+1)-2j,2i}(z-c_2)^{2i}(\rho-c_1)^{n(n+1)-2j}, \quad (56)\end{aligned}$$

where $b_{p,q}$ $(p,q=0,2,4,\dots,j(j+1))$ are constants that will be found later and c_1 and c_2 are real center controlling parameters of rogue wave.

For first order rogue wave solution, the auxiliary function $g(\rho,z)$ can be considered in the following form:

$$g(\rho,z)=b_{0,0}+b_{0,2}z^2+b_{2,0}\rho^2. \quad (57)$$

By substituting Eq. (57) into Eq. (55) and equating the coefficient of different powers of $\rho^i z^j$ to zero, we obtain a system of equations as

$$2\alpha\,b_{2,0}\,b_{0,2}-2\delta\,b_{0,2}^2+2d\,b_{2,0}\,b_{0,2}+2a\,b_{2,0}\,b_{0,2}-2b_{2,0}\,b_{0,2}=0, \quad (58a)$$

$$-2\alpha\,b_{2,0}^2-2d\,b_{2,0}^2+2\delta\,b_{0,2}\,b_{2,0}-2a\,b_{2,0}^2+2b_{2,0}^2=0, \quad (58b)$$

$$2b_{0,0}\,b_{2,0}(a+\alpha+d-1)+2\delta b_{0,0}\,b_{0,2}-12b_{2,0}^2=0. \quad (58c)$$

Furthermore, solving system of equation Eq. (58), we derive parametric values as

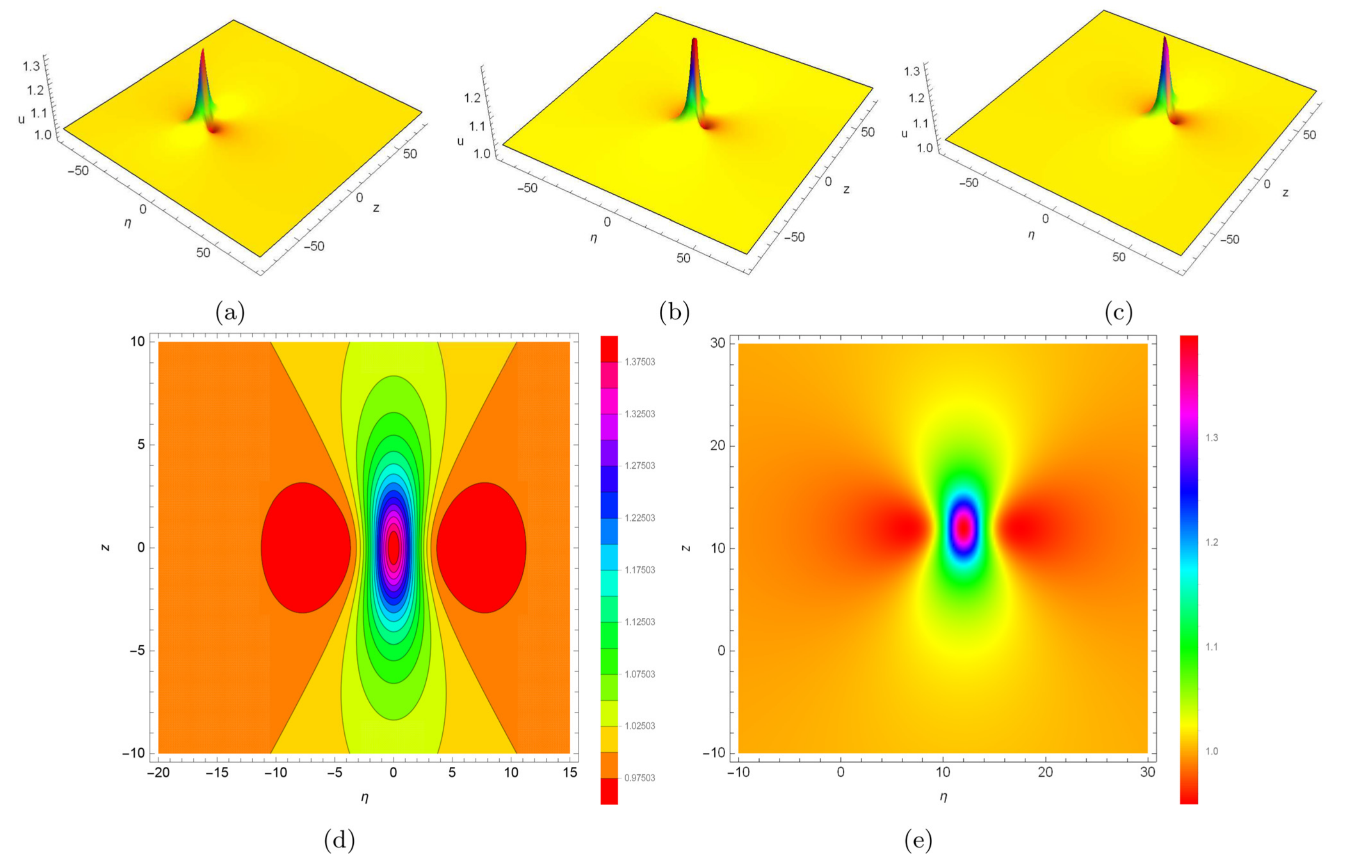

FIG. 7. First order rogue wave of Eq. (2) given by Eq. (61) with center controlling parameters as (a) $c_1 = -20,\ c_2 = -16$, (b) $c_1 = 0,\ c_2 = 0$, (c) $c_1 = 12,\ c_2 = 12$, (d) contour plot, and (e) density plot.

$$b_{2,0} = b_{2,0}, \quad b_{0,2} = \frac{b_{2,0}(a+\alpha+d-1)}{\delta}, \quad b_{0,0} = \frac{3b_{2,0}}{a+\alpha+d-1}. \tag{59}$$

With the parametric values in Eq. (59), Eq. (57) becomes

$$g(\rho,z) = \tilde{g}_1(\rho,z,c_1,c_2) = b_{2,0}\left(\frac{(a+\alpha+d-1)}{\delta}(z-c_2)^2 + (\rho-c_1)^2 + \frac{3}{a+\alpha+d-1}\right). \tag{60}$$

Finally, substitution of Eq. (60) into Eq. (54) yields first order rogue wave of Eq. (2) as

$$u(\rho,z) = -\frac{6}{b}\left[\log\left(b_{2,0}\left(\frac{(a+\alpha+d-1)}{\delta}(z-c_2)^2 + (\rho-c_1)^2 + \frac{3}{a+\alpha+d-1}\right)\right)\right]_{\rho\rho}. \tag{61}$$

In Fig. 7, we demonstrate evolution of rogue wave solution of Eq. (2) corresponding to the parametric values $\alpha = 0.5,\ \delta = 0.3,\ a = 0.5,\ b = 1,\ c = -1,\ d = 0.3,$ and $b_{2,0} = 1$.

VIII. LUMP SOLUTION

The lump solution[74,85] of Eq. (2) can be constructed by choosing the test function in the following form:

$$f = h_1^2 + h_2^2 + m_1, \tag{62}$$

where

$$h_1 = d_1x + d_2y + d_3z + d_4t + d_5, \tag{63a}$$

$$h_2 = d_6x + d_7y + d_8z + d_9y + d_{10}, \tag{63b}$$

where $m_1,\ d_i,\ (i = 1, 2, \ldots, 10)$ are constants that will be determined later, and the constants $d_i (i = 1, 2, 3, 6, 7, 8)$ satisfy the condition $(d_1, d_2, d_3) \nparallel (d_6, d_7, d_8)$. Substituting Eq. (61) into Eq. (20) and setting all the coefficient of different powers of $x^p y^q z^r t^s$ to zero, we obtain a system of equations. After solving the obtained system of equations with $\gamma = 1,\ \delta = \frac{1}{4d}$, we derive the following restriction between the parameters:

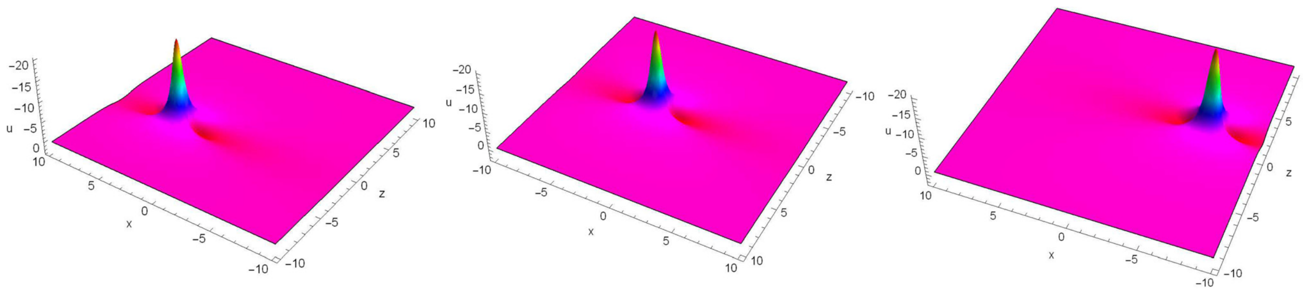

(a) (b) (c)

FIG. 8. Evolution of negative lump wave of Eq. (2) at (a) $t = -1.5$, (b) $t=0$, and (c) $t=1$.

$$d_2 = \frac{d_6 d_7}{d_1}, \quad d_3 = -\frac{d_6 d_8}{d_1}, \quad d_4 = \frac{4dd_6(\alpha d_7 + \beta d_8) - 4d(ad_1^2 - d\, d_7^2) + 4d\, d_8 d_7 + d_8^2}{4d\, d_1}, \quad m_1 = -\frac{12d\, cd_1^2(d_1^2 + d_6^2)}{(2d\, d_7 + d_8)^2}, \tag{64a}$$

$$d_9 = -\frac{4d\, d_1^2(\alpha d_7 + \beta d_8) + 4d\, d_6(ad_1^2 - dd_7^2) - (4d\, d_6 d_7 d_8 + d_6 d_8^2)}{d_1^2}, \quad d_{10} = \frac{d_5 d_6}{d_1}, \quad d_8 \neq -2d\, d_7, \quad c < 0. \tag{64b}$$

Finally, substituting Eq. (61) along with Eq. (64) into Eq. (20), we can derive lump solution of Eq. (2).

In Fig. 8, we demonstrate evolution of negative lump wave solution of Eq. (2) corresponding to the parametric values $a = b = d = \alpha = \beta = 1, \ c = -2, \ d_1 = 1, \ d_5 = 2, \ d_6 = 2, \ d_7 = 1,$ and $d_8 = 2.5$.

IX. LUMP-MULTI-STRIPE SOLUTION

To construct lump-multi-stripe solution from Hirota bilinear form Eq. (20) of Eq. (2), we can consider the test function f in a combined form of quadratic function and exponential function as

$$f = h_1^2 + h_2^2 + m_1 + \sum_{i=1}^{n} e^{\Upsilon_i}, \tag{65}$$

where $\Upsilon_i = k_i(x + p_i y + q_i z + w_i t) + \Upsilon_i^0, \ \ (i = 1, 2, 3, n), \ m_1 > 0$ and h_1 and h_2 are defined in Eq. (63).

The test function f in Eq. (65) can provide lump-multi-stripe solution[81] of Eq. (2) if and only if

$$(D_x D_t + aD_x^2 + cD_x^4 + dD_y^2 + \alpha D_x D_y + \beta D_x D_z + \gamma D_y D_z + \delta D_z^2)(h_1^2 + h_2^2 + m_1) \cdot (h_1^2 + h_2^2 + m_1) = 0, \tag{66a}$$

$$\left(D_x D_t + aD_x^2 + cD_x^4 + dD_y^2 + \alpha D_x D_y + \beta D_x D_z + \gamma D_y D_z + \delta D_z^2\right)(h_1^2 + h_2^2 + m_1) \cdot e^{\Upsilon_i}, \quad (i = 1, 2, \ldots, n), \tag{66b}$$

$$\left(D_x D_t + aD_x^2 + cD_x^4 + dD_y^2 + \alpha D_x D_y + \beta D_x D_z + \gamma D_y D_z + \delta D_z^2\right) (k_i - k_j, p_i - p_j, q_i - q_j, w_i - w_j) = 0, \quad (i \neq j, \ i, j = 1, 2, \ldots, n). \tag{66c}$$

Setting $\gamma = 1, \ \delta = \frac{1}{4d}$ and solving system of equations Eq. (66), we derive relation between parameters $m_1, d_i, (i = 1, 2, \ldots, 10)$ and $k_i, p_i, q_i, w_i \ (i = 1, 2, \ldots, n)$ as

$$d_2 = \frac{d_6 d_7}{d_1}, \quad d_3 = -\frac{d_6 d_8}{d_1}, \quad d_4 = \frac{4dd_6(\alpha d_7 + \beta d_8) - 4d(ad_1^2 - d\, d_7^2) + 4d\, d_8 d_7 + d_8^2}{4d\, d_1}, \quad m_1 = -\frac{12d\, cd_1^2(d_1^2 + d_6^2)}{(2d\, d_7 + d_8)^2}, \tag{67a}$$

$$d_9 = -\frac{4d\, d_1^2(\alpha d_7 + \beta d_8) + 4d\, d_6(ad_1^2 - dd_7^2) - (4d\, d_6 d_7 d_8 + d_6 d_8^2)}{d_1^2}, \quad d_{10} = \frac{d_5 d_6}{d_1}, \quad d_8 \neq -2d\, d_7, \quad c < 0, \tag{67b}$$

$$w_i = -\left(a + c k_i^2 + d p_i^2 + \alpha p_i + \beta q_i + p_i q_i + \frac{1}{4d} q_i^2\right), \ (i = 1, 2, \ldots, n). \tag{67c}$$

Then, the lump-multi-stripe solution of Eq. (2) is obtained as

$$u = \frac{6c}{b}\left[\log\left(h_1^2 + h_2^2 + m_1 + \sum_{i=1}^{n} e^{\Upsilon_i}\right)\right]_{xx}, \tag{68}$$

where

$$h_1 = d_1 x + \left(\frac{d_6 d_7}{d_1}\right) y + \left(-\frac{d_6 d_8}{d_1}\right) z + \left(\frac{4dd_6(\alpha d_7 + \beta d_8) - 4d(ad_1^2 - d\, d_7^2) + 4d\, d_8 d_7 + d_8^2}{4d\, d_1}\right) t + d_5, \tag{69a}$$

$$h_2 = d_6 x + d_7 y + d_8 z + \left(-\frac{4d\, d_1^2(\alpha d_7 + \beta d_8) + 4d\, d_6(ad_1^2 - dd_7^2) - (4d\, d_6 d_7 d_8 + d_6 d_8^2)}{d_1^2}\right) t + \frac{d_5 d_6}{d_1}, \tag{69b}$$

$$m_1 = -\frac{12d\, cd_1^2(d_1^2 + d_6^2)}{(2d\, d_7 + d_8)^2}, \tag{69c}$$

$$\Upsilon_i = k_i\left(x + p_i y + q_i z - \left(a + c k_i^2 + d p_i^2 + \alpha p_i + \beta q_i + p_i q_i + \frac{1}{4d} q_i^2\right) t\right) + \Upsilon_i^0, \quad (i = 1, 2, \ldots, n). \tag{69d}$$

A. Lump-one-stripe solution

For lump-one-stripe solution of Eq. (2), we take $i = 1$ in Eq. (68) and obtain lump-one-stripe solution as

$$u = \frac{6c}{b}\left[\log\left(h_1^2 + h_2^2 + m_1 + \sum_{i=1}^{n} e^{\Upsilon_1}\right)\right]_{xx}, \tag{70}$$

where

$$h_1 = d_1 x + \left(\frac{d_6 d_7}{d_1}\right) y + \left(-\frac{d_6 d_8}{d_1}\right) z + \left(\frac{4dd_6(\alpha d_7 + \beta d_8) - 4d(ad_1^2 - d\, d_7^2) + 4d\, d_8 d_7 + d_8^2}{4d\, d_1}\right) t + d_5, \tag{71a}$$

$$h_2 = d_6 x + d_7 y + d_8 z + \left(-\frac{4d\, d_1^2(\alpha d_7 + \beta d_8) + 4d\, d_6(ad_1^2 - dd_7^2) - (4d\, d_6 d_7 d_8 + d_6 d_8^2)}{d_1^2}\right) t + \frac{d_5 d_6}{d_1}, \tag{71b}$$

$$m_1 = -\frac{12d\, cd_1^2(d_1^2 + d_6^2)}{(2d\, d_7 + d_8)^2}, \tag{71c}$$

$$\Upsilon_1 = k_1\left(x + p_1 y + q_1 z - \left(a + c k_1^2 + d p_1^2 + \alpha p_1 + \beta q_1 + p_1 q_1 + \frac{1}{4d} q_1^2\right) t\right) + \Upsilon_1^0. \tag{71d}$$

In Fig. 9, we demonstrate interaction phenomena of negative lump wave with stripe wave and their evolution at different time frames corresponding to the parametric values as $a = b = d = \alpha = \beta = 1$, $c = -1$, $d_1 = 1$, $d_5 = 1$, $d_6 = 2$, $d_7 = 1$, $d_8 = 1.2$, $k_1 = 2$, $p_1 = 2$, $q_1 = 0.25$, and $\Upsilon_1^0 = 0$. At $t = -1.5$, there is only one stripe wave. Lump wave originates from stripe wave at $t = 0$. Then, at $t = 0.5$, lump wave separates from stripe wave and move on.

B. Lump-two-stripe solution

For lump-two-stripe solution of Eq. (2), we take $i = 2$ in Eq. (68) and obtain lump-two-stripe solution as

$$u = \frac{6c}{b}\left[\log\left(h_1^2 + h_2^2 + m_1 + e^{\Upsilon_1} + e^{\Upsilon_2}\right)\right]_{xx}, \tag{72}$$

where

$$h_1 = d_1 x + \left(\frac{d_6 d_7}{d_1}\right) y + \left(-\frac{d_6 d_8}{d_1}\right) z + \left(\frac{4dd_6(\alpha d_7 + \beta d_8) - 4d(ad_1^2 - d\, d_7^2) + 4d\, d_8 d_7 + d_8^2}{4d\, d_1}\right) t + d_5, \tag{73a}$$

$$h_2 = d_6 x + d_7 y + d_8 z + \left(-\frac{4d\, d_1^2(\alpha d_7 + \beta d_8) + 4d\, d_6(ad_1^2 - dd_7^2) - (4d\, d_6 d_7 d_8 + d_6 d_8^2)}{d_1^2}\right) t + \frac{d_5 d_6}{d_1}, \tag{73b}$$

$$m_1 = -\frac{12d\, cd_1^2(d_1^2 + d_6^2)}{(2d\, d_7 + d_8)^2}, \tag{73c}$$

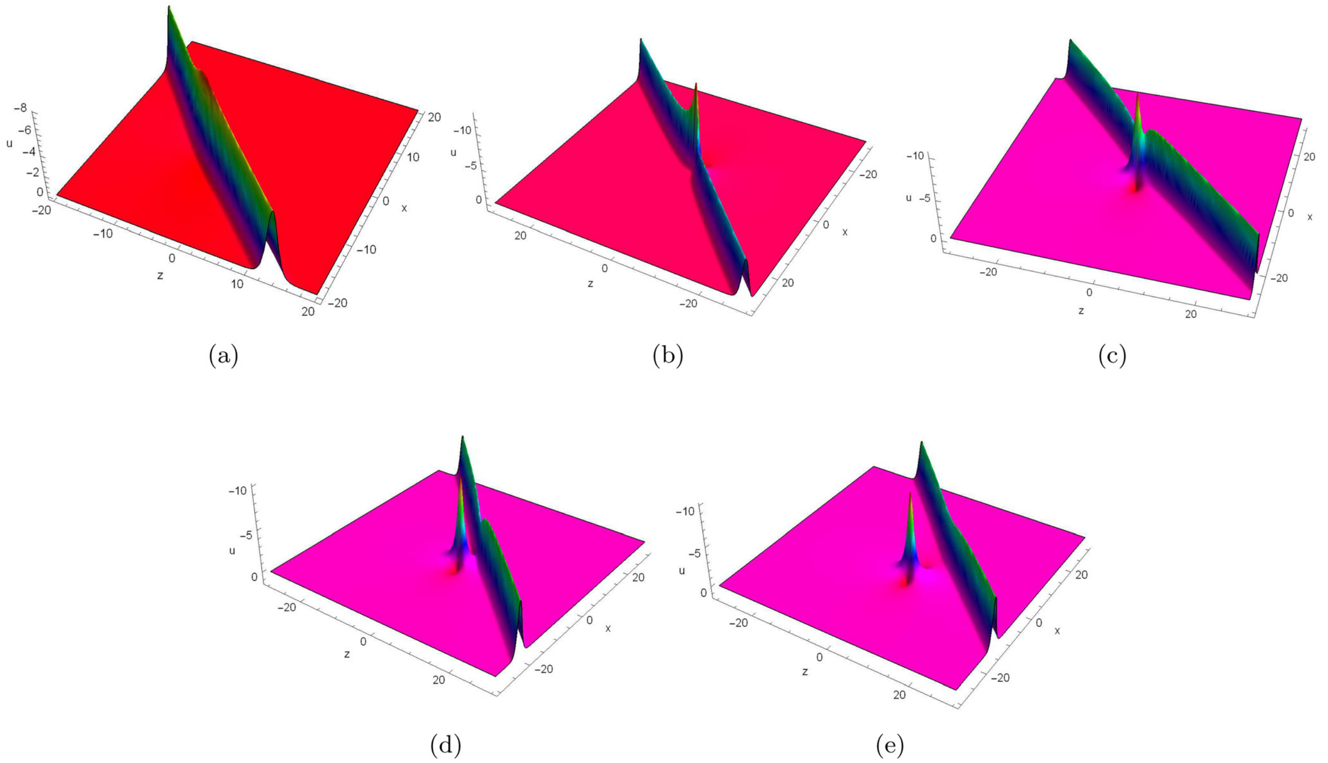

FIG. 9. Evolution of negative lump-one-stripe solution of Eq. (2) at (a) $t=-1.5$, (b) $t=-0.5$, (c) $t=0$, (d) $t=0.5$, and (e) $t=1.5$.

$$\Upsilon_i = k_i\left(x + p_i y + q_i z - \left(a + c\,k_i^2 + d\,p_i^2 + \alpha\,p_i + \beta\,q_i + p_i q_i + \frac{1}{4d}q_i^2\right)t\right) + \Upsilon_i^0, \quad (i=1,2). \tag{73d}$$

In Fig. 10, we demonstrate evolution of lump-two-stripe solution of Eq. (2) corresponding to the parametric values as $a=b=d=\alpha=\beta=1$, $c=-1$, $d_1=1$, $d_5=1$, $d_6=2$, $d_7=1$, $d_8=1.2$, $k_1=2$, $p_1=2$, $q_1=0.25$, $k_2=1$, $p_2=1$, $q_2=0.25$, and $\Upsilon_i^0=0$, $(i=1,2)$. At $t=-1.5$, there is only one stripe wave, and lump wave originates from stripe wave at $t=0$. Lump wave completely isolates from stripe wave at $t=2$. At $t=3.5$, stripe wave splits into two distinct stripe waves and then move on.

X. LUMP-MULTI-SOLITON SOLUTION

To construct a lump-multi-soliton solution from Hirota bilinear form Eq. (20) of Eq. (2), we can consider the test function f in a combined form of quadratic function and hyperbolic cosine function as

$$f = h_1^2 + h_2^2 + m_1 + \sum_{i=1}^{n}\cosh\Upsilon_i + m_2, \tag{74}$$

where $\Upsilon_i = k_i(x + p_i y + q_i z + w_i t) + \Upsilon_i^0$, $(i=1,2,3,n)$, $m_1, m_2 > 0$, and h_1 and h_2 are defined in Eq. (63).

The test function f in Eq. (74) can provide lump-multi-soliton solution[81] of Eq. (2) if and only if

$$\left(D_xD_t + aD_x^2 + cD_x^4 + dD_y^2 + \alpha D_xD_y + \beta D_xD_z + \gamma D_yD_z + \delta D_z^2)(h_1^2 + h_2^2 + m_1\right)\cdot(h_1^2 + h_2^2 + m_1) = 0, \tag{75a}$$

$$\left(D_xD_t + aD_x^2 + cD_x^4 + dD_y^2 + \alpha D_xD_y + \beta D_xD_z + \gamma D_yD_z + \delta D_z^2\right)(h_1^2 + h_2^2 + m_1)\cdot e^{\Upsilon_i}, \quad (i=1,2,\ldots,n), \tag{75b}$$

$$\begin{aligned}&\left(D_xD_t + aD_x^2 + cD_x^4 + dD_y^2 + \alpha D_xD_y + \beta D_xD_z + \gamma D_yD_z + \delta D_z^2)(h_1^2 + h_2^2 + m_1\right)\cdot m_2\\ &+ \sum_{i=1}^{n}\frac{1}{4}\left(D_xD_t + aD_x^2 + cD_x^4 + dD_y^2 + \alpha D_xD_y + \beta D_xD_z + \gamma D_yD_z + \delta D_z^2\right)(2k_i, 2p_i, 2q_i, 2w_i) = 0,\end{aligned} \tag{75c}$$

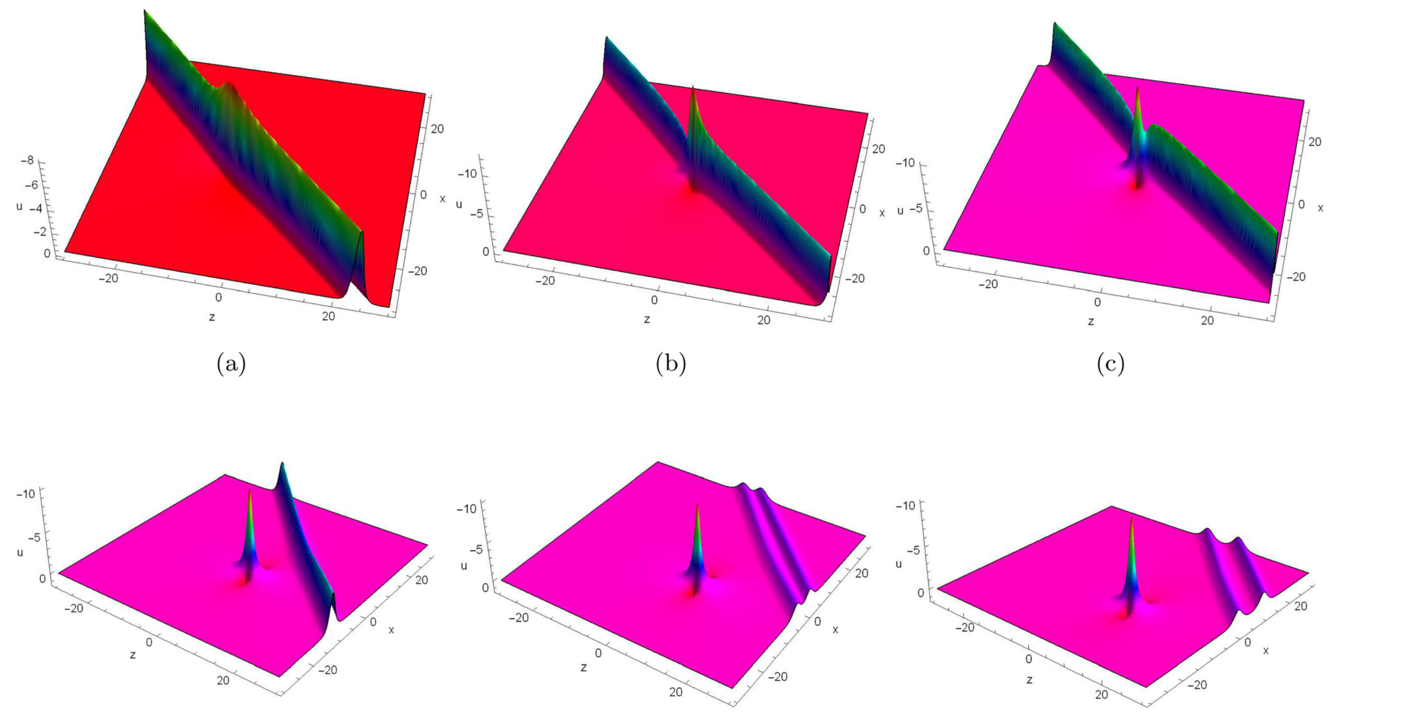

(a) (b) (c)

(d) (e) (f)

FIG. 10. Evolution of negative lump-two-stripe solution of Eq. (2) at (a) $t=-1.5$, (b) $t=-0.5$, (c) $t=0$, (d) $t=2$, (e) $t=3.5$, and (f) $t=4.5$.

$$\left(D_xD_t + aD_x^2 + cD_x^4 + dD_y^2 + \alpha D_xD_y + \beta D_xD_z + \gamma D_yD_z + \delta D_z^2\right)(k_i - k_j, p_i - p_j, q_i - q_j, w_i - w_j) = 0, \quad (i \neq j,\ i,j = 1,2,\ldots,n), \tag{75d}$$

$$\left(D_xD_t + aD_x^2 + cD_x^4 + dD_y^2 + \alpha D_xD_y + \beta D_xD_z + \gamma D_yD_z + \delta D_z^2\right)(k_i + k_j, p_i + p_j, q_i + q_j, w_i + w_j) = 0, \quad (i \neq j,\ i,j = 1,2,\ldots,n). \tag{75e}$$

Setting $\gamma = 1,\ \delta = \frac{1}{4d}$ and solving system of equations Eq. (75), we derive same relations between parameters $m_1,\ d_i, (i = 1, 2, \ldots, 10)$ and $k_i, p_i, q_i, w_i\ (i = 1, 2, \ldots, n)$ as in Eq. (67).

Then, the lump-multi-soliton solution of Eq. (2) is obtained as

$$u = \frac{6c}{b}\left[\log\left(h_1^2 + h_2^2 + m_1 + \sum_{i=1}^{n}\cosh\Upsilon_i + m_2\right)\right]_{xx}, \tag{76}$$

where

$$h_1 = d_1x + \left(\frac{d_6d_7}{d_1}\right)y + \left(-\frac{d_6d_8}{d_1}\right)z + \left(\frac{4dd_6(\alpha d_7 + \beta d_8) - 4d(ad_1^2 - d\,d_7^2) + 4d\,d_8d_7 + d_8^2}{4d\,d_1}\right)t + d_5, \tag{77a}$$

$$h_2 = d_6x + d_7y + d_8z + \left(-\frac{4d\,d_1^2(\alpha d_7 + \beta d_8) + 4d\,d_6(ad_1^2 - dd_7^2) - (4d\,d_6d_7d_8 + d_6d_8^2)}{d_1^2}\right)t + \frac{d_5d_6}{d_1}, \tag{77b}$$

$$m_1 = -\frac{12d\,cd_1^2(d_1^2 + d_6^2)}{(2d\,d_7 + d_8)^2}, \tag{77c}$$

$$\Upsilon_i = k_i\left(x + p_iy + q_iz - \left(a + c\,k_i^2 + d\,p_i^2 + \alpha\,p_i + \beta\,q_i + p_iq_i + \frac{1}{4d}q_i^2\right)t\right) + \Upsilon_i^0, \quad (i = 1, 2, \ldots, n). \tag{77d}$$

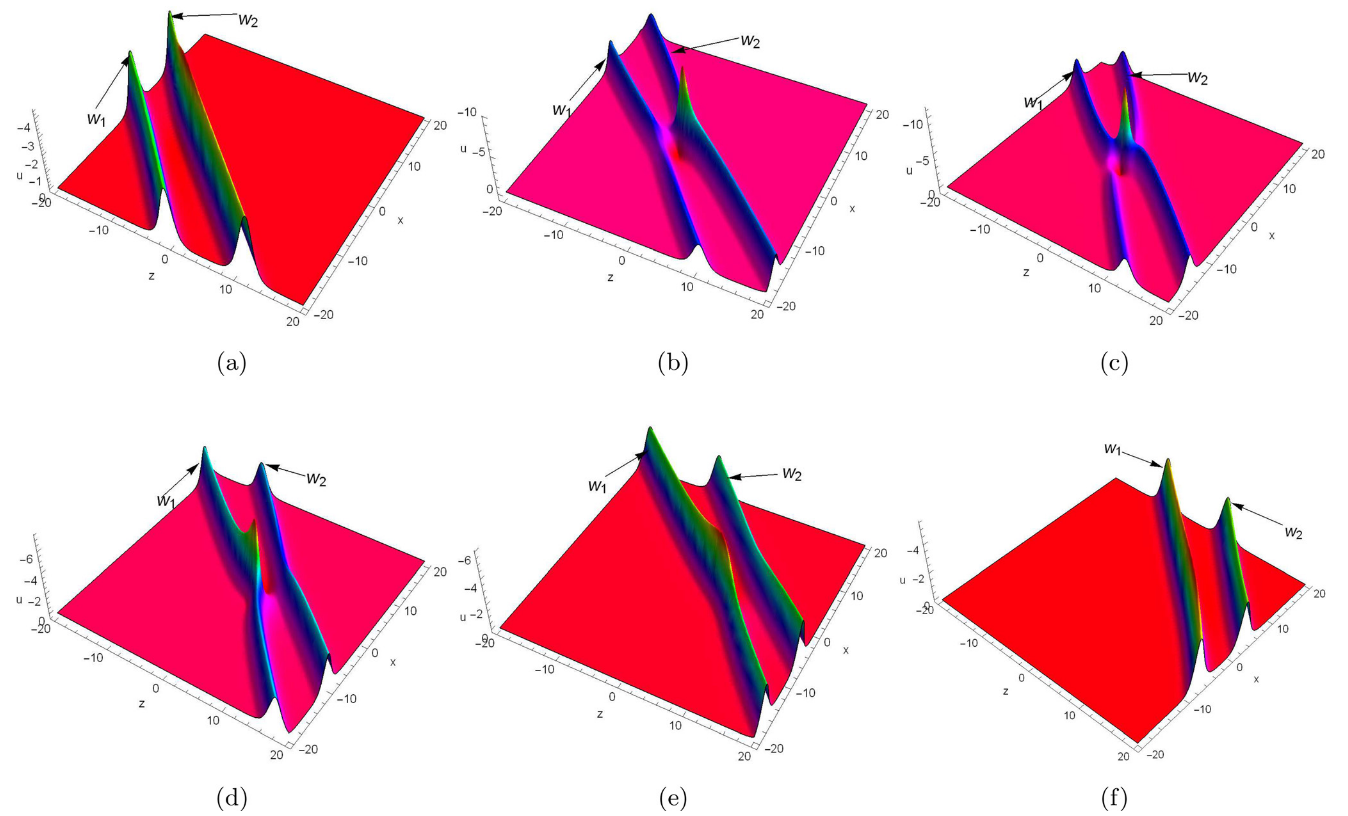

FIG. 11. Evolution of negative lump-one-soliton solution of Eq. (2) given by Eq. (78) at (a) $t = -4$, (b) $t = -1$, (c) $t = -0.3$, (d) $t = 1$, (e) $t = 2.3$, and (f) $t = 4.8$.

A. Lump-one-soliton solution

For lump-one-soliton solution of Eq. (2), we take $i = 1$ in Eq. (76) and obtain lump-one-soliton solution as

$$u = \frac{6c}{b}\left[\log\left(h_1^2 + h_2^2 + m_1 + \cosh\Upsilon_1 + m_2\right)\right]_{xx}, \tag{78}$$

where

$$h_1 = d_1 x + \left(\frac{d_6 d_7}{d_1}\right)y + \left(-\frac{d_6 d_8}{d_1}\right)z + \left(\frac{4dd_6(\alpha d_7 + \beta d_8) - 4d(ad_1^2 - d\,d_7^2) + 4d\,d_8 d_7 + d_8^2}{4d\,d_1}\right)t + d_5, \tag{79a}$$

$$h_2 = d_6 x + d_7 y + d_8 z + \left(-\frac{4d\,d_1^2(\alpha d_7 + \beta d_8) + 4d\,d_6(ad_1^2 - dd_7^2) - (4d\,d_6 d_7 d_8 + d_6 d_8^2)}{d_1^2}\right)t + \frac{d_5 d_6}{d_1}, \tag{79b}$$

$$m_1 = -\frac{12d\,cd_1^2(d_1^2 + d_6^2)}{(2d\,d_7 + d_8)^2}, \tag{79c}$$

$$\Upsilon_1 = k_1\left(x + p_1 y + q_1 z - \left(a + c\,k_1^2 + d\,p_1^2 + \alpha\,p_1 + \beta\,q_1 + p_1 q_1 + \frac{1}{4d}q_1^2\right)t\right) + \Upsilon_1^0. \tag{79d}$$

In Fig. 11, we illustrate the evolution of negative lump-one-soliton solution of Eq. (2) at different time frames corresponding to the parametric values as $a = b = d = \alpha = \beta = 1, c = -1, d_1 = 1,\ d_5 = 1, d_6 = 2, d_7 = 1, d_8 = 1.3, k_1 = 1.5, p_1 = 1, q_1 = 0.25, m_2 = 0,$ and $\Upsilon_1^0 = 0$. At $t = -4$, there are two solitary waves w_1 and w_2. Lump wave originates from w_2 at $t = -1$ and then disappears into wave w_1 with time.

B. Lump-two-soliton solution

For lump-two-soliton solution of Eq. (2), we take $i = 2$ in Eq. (76) and obtain lump-two-soliton solution as

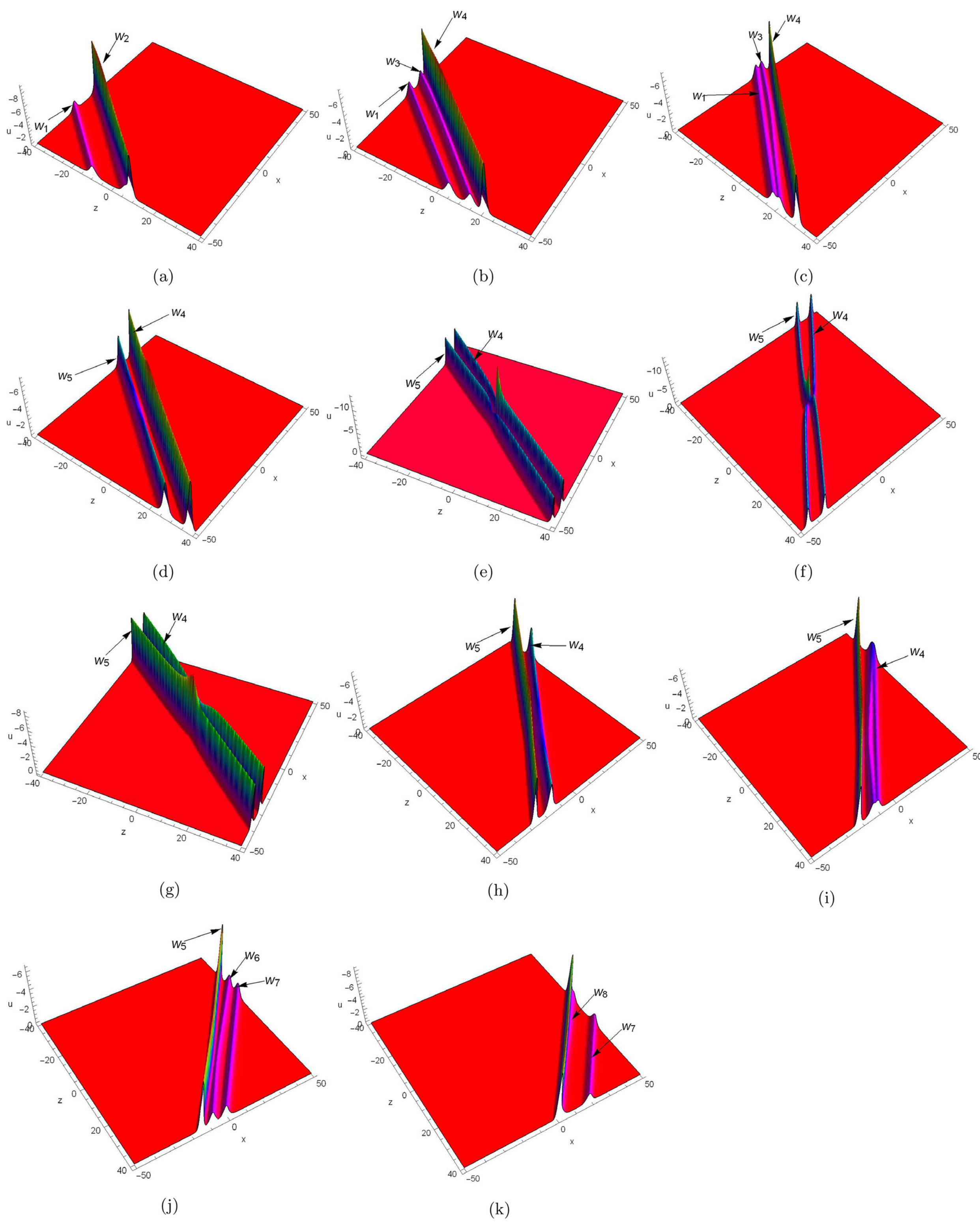

FIG. 12. Evolution of negative lump-two-soliton solution of Eq. (2) given by Eq. (80) at (a) $t = -6.7$, (b) $t = -5$, (c) $t = -3.6$, (d) $t = -2.6$, (e) $t = -0.5$, (f) $t = 0$, (g) $t = 1$, (h) $t = 2.7$, (i) $t = 3.3$, (j) $t = 4.3$, and (k) $t = 6.5$.

$$u = \frac{6c}{b}\left[\log\left(h_1^2 + h_2^2 + m_1 + \cosh\Upsilon_1 + \cosh\Upsilon_2 + m_2\right)\right]_{xx}, \tag{80}$$

where

$$h_1 = d_1 x + \left(\frac{d_6 d_7}{d_1}\right)y + \left(-\frac{d_6 d_8}{d_1}\right)z + \left(\frac{4dd_6(\alpha d_7 + \beta d_8) - 4d(ad_1^2 - d\,d_7^2) + 4d\,d_8 d_7 + d_8^2}{4d\,d_1}\right)t + d_5, \tag{81a}$$

$$h_2 = d_6 x + d_7 y + d_8 z + \left(-\frac{4d\,d_1^2(\alpha d_7 + \beta d_8) + 4d\,d_6(ad_1^2 - dd_7^2) - (4d\,d_6 d_7 d_8 + d_6 d_8^2)}{d_1^2}\right)t + \frac{d_5 d_6}{d_1}, \tag{81b}$$

$$m_1 = -\frac{12d\,cd_1^2(d_1^2 + d_6^2)}{(2d\,d_7 + d_8)^2}, \tag{81c}$$

$$\Upsilon_i = k_i\left(x + p_i y + q_i z - \left(a + c\,k_i^2 + d\,p_i^2 + \alpha\,p_i + \beta\,q_i + p_i q_i + \frac{1}{4d}q_i^2\right)t\right) + \Upsilon_i^0, \quad (i = 1, 2). \tag{81d}$$

In Fig. 12, we illustrate the evolution of negative lump-two-soliton solution of Eq. (2) corresponding to the parametric values as $a = b = d = \alpha = \beta = 1$, $c = -1$, $d_1 = 1$, $d_5 = 1$, $d_6 = 2$, $d_7 = 1$, $d_8 = 1.3$, $k_1 = 1.5$, $p_1 = 2$, $q_1 = 0.25$, $k_2 = 1$, $p_2 = 1$, $q_2 = 0.25$, $m_2 = 0$, and $\Upsilon_i^0 = 0$ $(i = 1, 2)$. Evolution of lump-two-soliton solution is more sophisticated due to the presence of various fissions and fusions of waves. At $t = -6.7$, exactly two waves w_1 and w_2 are appeared. Then, at $t = -5$, wave w_2 starts splitting to w_3 and w_4, and at $t = -3.6$, it completely splits because of the fission effect. At $t = -2.6$, wave w_5 appears as a result of the fusion effect of waves w_1 and w_3. At $t = -0.5$, lump wave originates from w_4 and completely disappears into wave w_5 at $t = 2.7$. Then, wave w_4 splits into w_6 and w_7. Finally, because of the fusion effect of w_5 and w_6, wave w_8 generates.

XI. GRAPHICAL ILLUSTRATION, RESULTS, AND DISCUSSION

In Fig. 1, we depict 3D plot, density plot, and 2D plot of one soliton solution of Eq. (2) corresponding to the parametric values as $a = c = d = \alpha = \beta = \gamma = \delta = 1$, $k_1 = 0.4$, $p_1 = 1.2$, $q_1 = 1.3$, and $\Upsilon_1^0 = 0$. Similarly, in Figs. 2 and 4, we present a 3D plot, density plot, and 2D plot of two soliton solutions and three soliton solution of Eq. (2), choosing parametric values as $a = c = d = \alpha = \beta = \gamma = \delta = 1$, $k_1 = 0.9$, $p_1 = 1.2$, $q_1 = 1.3$, $k_2 = -1.3$, $p_2 = 0.7$, $q_2 = 2$, and $\Upsilon_i^0 = 0$ $(i = 1, 2)$ and $a = c = d = \alpha = \beta = \gamma = \delta = 1$, $k_1 = 0.9$, $p_1 = 1.2$, $q_1 = 1.3$, $k_2 = -1.3$, $p_2 = 0.7$, $q_2 = 2$, $k_3 = 1.7$, $p_3 = 1$, $q_3 = 1.7$, and $\Upsilon_i^0 = 0$ $(i = 1, 2, 3)$, respectively. Figures 3 and 5 show the propagation of two soliton solution and three soliton solution of the model equation. Notably, larger solitary waves collide elastically with smaller waves, and after the nonlinear interaction, all waves retain their shapes asymptotically. The larger waves continue moving ahead of the smaller ones, demonstrating that the soliton solutions maintain their original shape and size with only a phase change during interaction. In Fig. 6, we illustrate the dynamical behavior of the solution given by Eq. (52) at different time frames. At the outset, waves appear from a constant state and progressively transform into periodic line waves. These periodic line waves maintain parallelism and independence from each other, yet their behaviors evolve consistently over time. In Fig. 7, we demonstrate 3D plots of first order rogue wave solution corresponding to the different center controlling parameters as $c_1 = -20$, $c_2 = -16$; $c_1 = 0$, $c_2 = 0$; and $c_1 = 12$, $c_2 = 12$. In Fig. 8, we present evolution of lump solution corresponding to the parametric values as $a = b = d = \alpha = \beta = 1$, $c = -2$, $d_1 = 1$, $d_5 = 2$, $d_6 = 2$, $d_7 = 1$, and $d_8 = 2.5$. Figure 9 depicts the evolutionary process of a lump solution emerging from a stripe solution. In the lump-one-stripe solution, a lump wave generates from a stripe wave and gradually separates from the stripe wave over time. Figure 10 illustrates the evolutionary process and fission effect of lump and stripe solutions. In the lump-two-stripe solution, a lump wave originates from the stripe wave, and subsequently, the lump and stripe waves separate after a certain duration. Following this separation, the stripe wave further divides into two distinct stripe waves. In Fig. 11, we illustrate the evolutionary process of a lump solution arising from a soliton solution, along with their interaction dynamics. In the lump-one-soliton solution, a lump wave emanates from one of the solitary waves, gradually detaches from that solitary wave and interacts with another solitary wave. After that, lump wave fades away entirely and transforms into another solitary wave over time. This indicates that the interaction between lump and one-soliton is entirely inelastic. Figure 12 depicts the occurrence of multiple fission and fusion effects in the evolution of a lump solution from soliton solutions. Within the lump-two-soliton solution, various instances of fission and fusion phenomena occur. Initially, there are only two solitary waves, denoted as w_1 and w_2. Subsequently, w_2 divides into two solitary waves, w_3 and w_4. Following this, w_3 interacts with w_1, giving rise to the formation of a new solitary wave, w_5. A lump wave originates from w_4, gradually separates from it, interacts with w_5, and eventually dissipates completely within w_5. Following this, w_5 splits into two solitary waves, w_6 and w_7. Again, w_6 interacts with w_5, resulting in the emergence of a new solitary wave, w_8. This suggests that the interaction between the lump and the two-soliton is also completely nonelastic.

XII. CONCLUSION

In this article, we have delved into the intricacies of the integrability characteristics inherent in a novel $(3+1)$-dimensional nonlinear evolution equation. Our approach commences with the elucidation of fundamental properties rooted in Bell polynomial theory. Leveraging this theoretical framework, we derive both the Hirota bilinear form and a bilinear Bäcklund transformation. By employing the Cole–Hopf transformation within the bilinear Bäcklund transformation and subsequently linearizing it, we arrive at the formulation of a Lax pair.

Furthermore, our exploration extends to the integrability aspect of the model equation, involving the derivation of an infinite sequence of conservation laws. The analytical effectiveness of the Hirota bilinear form facilitates the derivation of one, two, and three soliton solutions, vividly portrayed through graphical representations. Beyond solitons, we delve into the realm of breather solutions, introducing complex conjugate parameters into the two-soliton solution and visually depicting their evolutionary patterns. Our exploration takes an intriguing turn as we derive a first-order center-controlled rogue wave solution, dynamically illustrating its behavior across varying center-controlling parameter values. Expanding the scope of our inquiry, we employ the well-established quadratic function as a test function within the Hirota bilinear form, resulting in the deduction of the lump solution. Furthermore, a novel approach utilizing a combined form of a quadratic function and an exponential function as a test function yields lump-multi-stripe solutions, capturing their evolutionary phenomena through graphical representations. Pushing the boundaries of our investigation, we delve into the synthesis of lump-multi-soliton solutions through the combined application of a quadratic function and hyperbolic cosine function as test functions. The visually compelling depictions of their evolutionary phenomena add another layer to our understanding of these complex nonlinear wave dynamics. Significantly, these discoveries enhance our understanding of nonlinear wave phenomena across diverse fields, including shallow water dynamics, oceanography, and nonlinear optics. The results derived from this analytical framework offer a valuable and precise method for interpreting and describing various intricate phenomena within these scientific domains. In future endeavors, our goal is to apply the linear superposition principle to the Hirota bilinear form within a complex field. This approach seeks to extract solutions in the form of complex exponential wave functions, giving rise to phenomena such as complexitons, resonant solitons, and related effects. Additionally, another avenue of our research will involve exploring symmetry reductions of exact solutions through Lie symmetry analysis.

ACKNOWLEDGMENTS

The author UKM wishes to express his gratitude to the CSIR for providing financial support in the form of an SRF scholarship, as evidenced by letter number 09/106(0198)/2019-EMR-I. The author AD gratefully acknowledges the financial support provided under the Scheme "Fund for Improvement of S & T Infrastructure (FIST)" of the Department of Science & Technology (DST), Government of India, as evidenced by letter number SR/FST/MS-I/2019/42 to the Department of Mathematics, University of Kalyani. The research work of AD is also funded by SERB-DST (Government of India), file no: EEQ/2022/000719.

AUTHOR DECLARATIONS

Conflict of Interest

The authors have no conflicts to disclose.

Author Contributions

Uttam Kumar Mandal: Conceptualization (equal); Methodology (equal); Software (equal); Writing—original draft (equal). **Amiya Das:** Formal analysis (lead); Resources (equal); Software (equal); Supervision (lead); Validation (lead); Visualization (lead); Writing—review & editing (lead). **Wen-Xiu Ma:** Formal analysis (equal); Supervision (equal); Visualization (equal); Writing—review & editing (equal).

DATA AVAILABILITY

All data generated or analyzed during this study are included in this article.

REFERENCES

[1]B. R. Munson, T. H. Okiishi, W. W. Huebsch, and A. P. Rothmayer, *Fundamentals of Fluid Mechanics* (Wiley, 2013).
[2]M. A. Abdou, "The extended F-expansion method and its application for a class of nonlinear evolution equations," Chaos Solitons Fractals **31**, 95–104 (2007).
[3]A. Kubokawa, "Growing solitary disturbance in a baroclinic boundary current," J. Phys. Oceanogr. **19**, 182–192 (1989).
[4]J. M. Luttinger and W. Kohn, "Motion of electrons and holes in perturbed periodic fields," Phys. Rev. **97**, 869 (1955).
[5]P. Gray and S. K. Scott, *Chemical Oscillations and Instabilities: Non-Linear Chemical Kinetics* (Oxford University Press, 1990).
[6]A. Hasegawa, *Plasma Instabilities and Nonlinear Effects* (Springer Science and Business Media, 2012).
[7]G. P. Agrawal, *Nonlinear Fiber Optics* (Academic Press, San Diego, 2006).
[8]C. S. Gardner, J. M. Greene, M. D. Kruskal, and R. M. Miura, "Method for solving the Korteweg-de Vries equation," Phys. Rev. Lett. **19**, 1095 (1967).
[9]S. Kumar, I. Hamid, and M. A. Abdou, "Dynamic frameworks of optical soliton solutions and soliton-like formations to Schrödinger–Hirota equation with parabolic law non-linearity using a highly efficient approach," Opt. Quant. Electron. **55**, 1261 (2023).
[10]Y. Chen and X. Lü, "Wronskian solutions and linear superposition of rational solutions to B-type Kadomtsev–Petviashvili equation," Phys. Fluids **35**, 106613 (2023).
[11]S. Rani, S. Kumar, and N. Mann, "On the dynamics of optical soliton solutions, modulation stability, and various wave structures of a $(2+1)$-dimensional complex modified Korteweg-de-Vries equation using two integration mathematical methods," Opt. Quant. Electron. **55**, 731 (2023).
[12]Y. H. Yin, X. Lü, R. Jiang, B. Jia, and Z. Gao, "Kinetic analysis and numerical tests of an adaptive car-following model for real-time traffic in ITS," Phys. A **635**, 129494 (2024).
[13]K. Liu, X. Lü, F. Gao, and J. Zhang, "Expectation-maximizing network reconstruction and most applicable network types based on binary time series data," Phys. D **454**, 133834 (2023).
[14]M. Niwas and S. Kumar, "Multi-peakons, lumps, and other solitons solutions for the $(2+1)$-dimensional generalized Benjamin–Ono equation: An inverse (G'/G)-expansion method and real-world applications," Nonlinear Dyn. **111**, 22499–22512 (2023).
[15]R. Hirota, *The Direct Method in Soliton Theory* (Cambridge University Press, Cambridge, 2004).
[16]M. J. Ablowitz, M. A. Ablowitz, and P. A. Clarkson, *Solitons, Nonlinear Evolution Equations and Inverse Scattering Transform* (Cambridge University Press, Cambridge, 1991).
[17]J. Weiss, M. Tabor, and G. Carnevale, "The Painlevè property for partial differential equations," J. Math. Phys. **24**, 522–526 (1983).
[18]A. M. Wazwaz, W. Alhejaili, R. T. Matoog, and S. A. El-Tantawy, "On the Painlevè integrability of three-extensions to Mikhailov–Novikov–Wang equations: Multiple solitons, shocks, and other physical solutions," Phys. Fluids **35**, 113114 (2023).
[19]Y. Q. Chen, B. Tian, Y. Shen, and T. Y. Zhou, "Painlevè integrable property, Bäcklund transformations, Lax pair, and soliton solutions of a $(3+1)$-dimensional variable-coefficient Hirota bilinear system in a fluid," Phys. Fluids **35**, 127107 (2023).
[20]R. F. Zhang, M. C. Li, J. Y. Gan, Q. Li, and Z. Z. Lan, "Novel trial functions and rogue waves of generalized breaking soliton equation via bilinear neural network method," Chaos Solitons Fractals **154**, 111692 (2022).

[21]Y. H. Yin, X. Lü, and W. X. Ma, "Bäcklund transformation, exact solutions and diverse interaction phenomena to a (3 + 1)-dimensional nonlinear evolution equation," Nonlinear Dyn. **108**, 4181–4194 (2022).

[22]R. F. Zhang and M. C. Li, "Bilinear residual network method for solving the exactly explicit solutions of nonlinear evolution equations," Nonlinear Dyn. **108**, 521–531 (2022).

[23]W. X. Ma and W. Strampp, "An explicit symmetry constraint for the Lax pairs and the adjoint Lax pairs of AKNS systems," Phys. Lett. A **185**, 277–286 (1994).

[24]V. B. Matveed and M. A. Salle, *Darboux Transformation and Solitons* (Springer-Verlag, Berlin, 1991).

[25]P. J. Olver, *Applications of Lie Groups to Differential Equations* (Springer, Berlin, 2000).

[26]S. Kumar and S. Rani, "Symmetries of optimal system, various closed-form solutions, and propagation of different wave profiles for the Boussinesq–Burgers system in ocean waves," Phys. Fluids **34**, 037109 (2022).

[27]S. Kumar, W. X. Ma, S. K. Dhiman, and A. Chauhan, "Lie group analysis with the optimal system, generalized invariant solutions, and an enormous variety of different wave profiles for the higher-dimensional modified dispersive water wave system of equations," Eur. Phys. J. Plus **138**, 434 (2023).

[28]J. Sirker, R. G. Pereira, and I. Affleck, "Conservation laws, integrability, and transport in one-dimensional quantum systems," Phys. Rev. B **83**, 035115 (2011).

[29]W. X. Ma, "Four-component integrable hierarchies of Hamiltonian equations with $(m+n+2)$ th-order Lax pairs," Theor. Math. Phys. **216**, 1180–1188 (2023).

[30]W. X. Ma, "Soliton solutions to constrained nonlocal integrable nonlinear Schrödinger hierarchies of type $(-\lambda, \lambda)$," Int. J. Geom. Methods Mod. Phys. **20**, 2350098 (2023).

[31]Y. Yang, T. Xia, and T. Liu, "Rational and semi-rational solutions of a (3 + 1)-dimensional generalized Calogero–Bogoyavlenskii–Schiff equation," Nonlinear Dyn. **111**, 16377–16394 (2023).

[32]A. Yokus and M. A. Isah, "Dynamical behaviors of different wave structures to the Korteweg-de Vries equation with the Hirota bilinear technique," Phys. A **622**, 128819 (2023).

[33]M. M. Liu, J. P. Yu, and W. X. Ma, "Dynamic analysis of lump solutions based on the dimensionally reduced generalized Hirota bilinear KP–Boussinesq equation," Mod. Phys. Lett. B **37**, 2250203 (2023).

[34]X. Wu, Y. Chen, and X. W. Yan, "General soliton, line breather and (semi)-rational solutions for the nonlocal long-wave-short-wave resonance interaction equation," Nonlinear Dyn. **112**, 661 (2023).

[35]S. Kumar and B. Mohan, "A generalized nonlinear fifth-order KdV-type equation with multiple soliton solutions: Painlevè analysis and Hirota bilinear technique," Phys. Scr. **97**, 125214 (2022).

[36]Y. Q. Chen, B. Tian, Y. Shen, and T. Y. Zhou, "Auto-Bäcklund transformations and analytic solutions of a generalized $(4+1)$-dimensional variable-coefficient Fokas equation for the shallow water waves," Phys. Fluids **35**, 077125 (2023).

[37]S. Kumar and B. Mohan, "A study of multi-soliton solutions, breather, lumps, and their interactions for Kadomtsev–Petviashvili equation with variable time coefficient using Hirota method," Phys. Scr. **96**, 125255 (2021).

[38]Y. Q. Chen, B. Tian, Y. Shen, and T. Y. Zhou, "Study on extensions of (modified) Korteweg-de Vries equations: Painlevè integrability and multiple soliton solutions in fluid mediums," Phys. Fluids **35**, 093110 (2023).

[39]S. Kumar, B. Mohan, and A. Kumar, "Generalized fifth-order nonlinear evolution equation for the Sawada–Kotera, Lax, and Caudrey–Dodd–Gibbon equations in plasma physics: Painlevè analysis and multi-soliton solutions," Phys. Scr. **97**, 035201 (2022).

[40]S. Kumar and B. Mohan, "A novel and efficient method for obtaining Hirota's bilinear form for the nonlinear evolution equation in $(n+1)$ dimensions," Partial Differ. Equ. Appl. Math. **5**, 100274 (2022).

[41]C. Gilson, F. Lambert, J. Nimmo, and R. Willox, "On the combinatorics of the Hirota D-operators," Proc. R. Soc. Lond., Ser. A **452**, 223–234 (1996).

[42]F. Lambert and J. Springael, "Construction of Bäcklund transformations with binary Bell Polynomials," J. Phys. Soc. Jpn. **66**, 2211–2213 (1997).

[43]F. Lambert and J. Springael, "On a direct procedure for the disclosure of Lax pairs and Bäcklund transformations," Chaos Solitons Fractals **12**, 2821–2832 (2001).

[44]E. Fan, "The integrability of nonisospectral and variable-coefficient KdV equation with binary Bell polynomials," Phys. Lett. A **375**, 493 (2011).

[45]S. Singh and S. Saha Ray, "Bilinear representation, bilinear Bäcklund transformation, Lax pair and analytical solutions for the fourth-order potential Ito equation describing water waves via Bell polynomials," J. Math. Anal. Appl. **530**, 127695 (2024).

[46]U. K. Mandal, S. Malik, S. Kumar, and A. Das, "A generalized (2 + 1)-dimensional Hirota bilinear equation: Integrability, solitons and invariant solutions," Nonlinear Dyn. **111**, 4593–4611 (2023).

[47]G. Q. Xu and A. M. Wazwaz, "A new $(n+1)$-dimensional generalized Kadomtsev–Petviashvili equation: Integrability characteristics and localized solutions," Nonlinear Dyn. **111**, 9495–9507 (2023).

[48]X. Lü and S. J. Chen, "N-soliton solutions and associated integrability for a novel (2 + 1)-dimensional generalized KdV equation," Chaos Solitons Fractals **169**, 113291 (2023).

[49]A. Das and U. K. Mandal, "Integrability, bilinearization, solitons and exact three wave solutions for a forced Korteweg-de Vries equation," Commun. Nonlinear Sci. Numer Simul. **102**, 105936 (2021).

[50]D. Gao, X. Lü, and M. S. Peng, "Study on the (2 + 1)-dimensional extension of Hietarinta equation: Soliton solutions and Bäcklund transformation," Phys. Scr. **98**, 095225 (2023).

[51]S. Singh and S. S. Ray, "Newly exploring the Lax pair, bilinear form, bilinear Bäcklund transformation through binary Bell polynomials, and analytical solutions for the (2 + 1)-dimensional generalized Hirota–Satsuma–Ito equation," Phys. Fluids **35**, 087134 (2023).

[52]C. Kharif, E. Pelinovsky, and A. Slunyaev, *Rogue Waves in the Ocean* (Springer, 2008).

[53]D. R. Solli, C. Ropers, P. Koonath, and B. Jalali, "Optical rogue waves," Nature **450**, 1054–1057 (2007).

[54]Y. V. Bludov, V. V. Konotop, and N. Akhmediev, "Vector rogue waves in binary mixtures of Bose–Einstein condensates," Eur. Phys. J. **185**, 169–180 (2010).

[55]V. B. Efimov, A. N. Ganshin, G. V. Kolmakov, P. V. E. McClintock, and L. P. M. Deglin, "Rogue waves in superfluid helium," Eur. Phys. J. **185**, 181–193 (2010).

[56]W. M. Moslem, P. K. Shukla, and B. Eliasson, "Surface plasma rogue waves," Europhys. Lett. **96**, 25002 (2011).

[57]M. Shats, H. Punzmann, and H. Xia, "Capillary rogue waves," Phys. Rev. Lett. **104**, 104503 (2010).

[58]M. Närhi, B. Wetzel, C. Billet, S. Toenger, T. Sylvestre, J. M. Merolla, R. Morandotti, F. Dias, G. Genty, and J. M. Dudley, "Real-time measurements of spontaneous breathers and rogue wave events in optical fibre modulation instability," Nat. Commun. **7**, 13675 (2016).

[59]Y. Z. Ya, "Financial rogue waves," Commun. Theor. Phys. **54**, 947 (2010).

[60]D. Y. Yang, B. Tian, and Y. Shen, "Generalized Darboux transformation and rogue waves for a coupled variable-coefficient nonlinear Schrödinger system in an inhomogeneous optical fiber," Chin. J. Phys. **82**, 182–193 (2023).

[61]X. Guan, H. Yang, X. Meng, and W. Liu, "Higher-order rogue waves solutions of the modified Gerdjikov–Ivanov equation with dispersion via generalized Darboux transformation," Appl. Math. Lett. **136**, 108466 (2023).

[62]N. Song, R. Liu, M. M. Guo, and W. X. Ma, "Nth order generalized Darboux transformation and solitons, breathers and rogue waves in a variable-coefficient coupled nonlinear Schrödinger equation," Nonlinear Dyn. **111**, 19347–19357 (2023).

[63]Y. Sun, J. Wu, and B. Li, "Rogue wave solutions of (3 + 1)-dimensional Kadomtsev–Petviashvili equation by a direct limit method," Commun. Theor. Phys. **75**, 065002 (2023).

[64]B. Wang, Z. Ma, and S. Xiong, "M-lump, rogue waves, breather waves, and interaction solutions among four nonlinear waves to new (3 + 1)-dimensional Hirota bilinear equation," Nonlinear Dyn. **111**, 9477–9494 (2023).

[65]S. T. R. Rizvi and S. Ahmed, "Resonant collisions among X-type, multi-lump, generalized breathers, N-solitons, and rogue waves in plasma," Optik **292**, 171390 (2023).

[66]Zhaqilao, "A symbolic computation approach to constructing rogue waves with a controllable center in the nonlinear systems," Comput. Math. Appl. **75**, 3331–3342 (2018).

[67]S. Kumar and B. Mohan, "A direct symbolic computation of center-controlled rogue waves to a new Painlevé-integrable (3 + 1)-D generalized nonlinear evolution equation in plasmas," Nonlinear Dyn. **111**, 16395–16405 (2023).

[68] Y. Liu and Y. Yang, "Rogue wave solutions for the (3 + 1)-dimensional generalized Camassa–Holm–Kadomtsev–Petviashvili equation," Chin. J. Phys. **86**, 508–514 (2023).
[69] B. Mohan, S. Kumar, and R. Kumar, "Higher-order rogue waves and dispersive solitons of a novel P-type (3 + 1)-D evolution equation in soliton theory and nonlinear waves," Nonlinear Dyn. **111**, 20275–20288 (2023).
[70] S. Kumar, B. Mohan, and R. Kumar, "Newly formed center-controlled rouge wave and lump solutions of a generalized (3 + 1)-dimensional KdV–BBM equation via symbolic computation approach," Phys. Scr. **98**, 085237 (2023).
[71] S. Kumar and B. Mohan, "A novel analysis of Cole–Hopf transformations in different dimensions, solitons, and rogue waves for a (2 + 1)-dimensional shallow water wave equation of ion-acoustic waves in plasmas," Phys. Fluids **35**, 127128 (2023).
[72] F. Fan and Z. Xu, "Breather and rogue wave solutions for the generalized discrete Hirota equation via Darboux–Bäcklund transformation," Wave Motion **119**, 103139 (2023).
[73] C. Lv, S. Shen, and Q. P. Liu, "Inverse scattering transform for the coupled modified complex short pulse equation: Riemann–Hilbert approach and soliton solutions," Phys. D **458**, 133986 (2024).
[74] W. X. Ma, "Lump solutions to the Kadomtsev–Petviashvili equation," Phys. Lett. A **379**, 1975–1978 (2015).
[75] A. M. Wazwaz, "Painlevè integrability and lump solutions for two extended (3 + 1) and (2 + 1)-dimensional Kadomtsev–Petviashvili equations," Nonlinear Dyn. **111**, 3623–3632 (2023).
[76] Y. Zhou, X. Zhang, C. Zhang, J. Jia, and W. X. Ma, "New lump solutions to a (3 + 1)-dimensional generalized Calogero–Bogoyavlenskii–Schiff equation," Appl. Math. Lett. **141**, 108598 (2023).
[77] H. Ma, S. Yue, Y. Gao, and A. Deng, "Lump solution, breather soliton and more soliton solutions for a (2 + 1)-dimensional generalized Benjamin–Ono equation," Qual. Theory Dyn. Syst. **22**, 72 (2023).
[78] W. X. Ma, "Lump waves in a spatial symmetric nonlinear dispersive wave model in (2 + 1)-dimensions," Mathematics **11**, 4664 (2023).
[79] S. Kumar, B. Mohan, and R. Kumar, "Lump, soliton, and interaction solutions to a generalized two-mode higher-order nonlinear evolution equation in plasma physics," Nonlinear Dyn. **110**, 693–704 (2022).
[80] S. J. Chen, Y. H. Yin, and X. Lü, "Elastic collision between one lump wave and multiple stripe waves of nonlinear evolution equations," Commun. Nonlinear Sci. Numer. Simul. **130**, 107205 (2024).
[81] X. Lü and S. J. Chen, "Interaction solutions to nonlinear partial differential equations via Hirota bilinear forms: One-lump-multi-stripe and one-lump-multi-soliton types," Nonlinear Dyn. **103**, 947–977 (2021).
[82] S. J. Chen and X. Lü, "Lump and lump-multi-kink solutions in the (3 + 1)-dimensions," Commun. Nonlinear Sci. Numer. Simul. **109**, 106103 (2022).
[83] U. K. Mandal, B. Karmakar, A. Das, and W. X. Ma, "Integrability, bilinearization, exact traveling wave solutions, lump and lump-multi-kink solutions of a (3 + 1)-dimensional negative order KdV–Calogero–Bogoyavlenskii–Schiff equation," Nonlinear Dyn. **112**, 4727 (2024).
[84] L. Akinyemi, "Shallow ocean soliton and localized waves in extended (2 + 1)-dimensional nonlinear evolution equations," Phys. Lett. A **463**, 128668 (2023).
[85] A. M. Wazwaz, W. Alhejaili, and S. A. El-Tantawy, "Analytical study on two new (3 + 1)-dimensional Painlvè integrable equations: Kink, lump, and multiple soliton solutions in fluid mediums," Phys. Fluids **35**, 093119 (2023).
[86] H. An, D. Feng, and H. Zhu, "General M-lump, high-order breather and localized interaction solutions to the 2 + 1-dimensional Sawada–Kotera equation," Nonlinear Dyn. **98**, 1275–1286 (2019).
[87] W. Peng, S. Tian, and T. T. Zhang, "Characteristics of the breather waves, lump waves, and semi-rational solutions in a generalized (2 + 1)-dimensional asymmetrical Nizhnik–Novikov–Veselov equation," Mod. Phys. Lett. B. **33**, 1950350 (2019).